

2013

Application Of Adaptive Extended Kalman Filtering Scheme To Improve The Efficiency Of A Groundwater Contaminant Transport Model

Elvis Boamah Addai
North Carolina Agricultural and Technical State University

Follow this and additional works at: <https://digital.library.ncat.edu/theses>

Recommended Citation

Addai, Elvis Boamah, "Application Of Adaptive Extended Kalman Filtering Scheme To Improve The Efficiency Of A Groundwater Contaminant Transport Model" (2013). *Theses*. 330.
<https://digital.library.ncat.edu/theses/330>

This Thesis is brought to you for free and open access by the Electronic Theses and Dissertations at Aggie Digital Collections and Scholarship. It has been accepted for inclusion in Theses by an authorized administrator of Aggie Digital Collections and Scholarship. For more information, please contact iyanna@ncat.edu.

Application of Adaptive Extended Kalman Filtering Scheme to Improve the Efficiency of a
Groundwater Contaminant Transport Model

Elvis Boamah Addai

North Carolina A&T State University

A thesis submitted to the graduate faculty
in partial fulfillment of the requirements for the degree of

MASTER OF SCIENCE

Department: Civil, Architectural and Environmental Engineering

Major: Civil Engineering

Major Professor: Dr. Shoou-Yuh Chang

Greensboro, North Carolina

2013

School of Graduate Studies
North Carolina Agricultural and Technical State University
This is to certify that the Master's Thesis of

Elvis Boamah Addai

has met the thesis requirements of
North Carolina Agricultural and Technical State University

Greensboro, North Carolina
2013

Approved by:

Dr. Shoou-Yuh Chang
Major Professor

Dr. Stephanie Luster-Teasley
Committee Member

Dr. Manoj K. Jha
Committee Member

Dr. Sameer Hamoush
Department Chair

Dr. Sanjiv Sarin
Dean, The Graduate School

© Copyright by
Elvis Boamah Addai
2013

Biographical Sketch

Elvis Boamah Addai was born in Kumasi, Ghana. His parents believed in the importance of education and did their best to provide good education for their children. After finishing high school, he decided to study Geomatic Engineering. He received his bachelor's degree from University of Mines and Technology, Ghana in 2009. He enrolled in the master's program in Civil and Environmental Engineering at North Carolina Agricultural and Technical State University in 2011. He is a candidate for the Master of Science degree in Civil Engineering.

Dedication

This thesis is dedicated to my father, who taught me that the best kind of knowledge to have is that which is learned for its own sake. It is also dedicated to my mother, who taught me that even the largest task can be accomplished if it is done one step at a time.

Acknowledgements

I would like to express my sincere gratitude to my advisor Dr. Shoou-Yuh Chang for the continuous support of my study for his patience and immense knowledge. Besides my advisor, I would like to thank the rest of my thesis committee Dr. Stephanie Luster-Teasley and Dr. Manoj K. Jha for their insightful comments. My sincere thanks also go to my family, friends and colleague graduate students for their support. This work was sponsored by the US Department of Energy's Samuel Massie Chair of Excellence Program under grant number DE-NA0000718.

Table of Contents

List of Figures	viii
List of Symbols	x
Abstract	2
CHAPTER 1 Introduction.....	3
CHAPTER 2 Literature Review	6
CHAPTER 3 Methodology.....	15
3.1 Deterministic Model.....	15
3.2 Numerical Solution Approach.....	16
3.3 Process Equation	18
3.4 Measurement Equation.....	18
3.5 Kalman Filter Algorithm.....	19
3.6 Extended Kalman Filter	20
3.7 Adaptive Extended Kalman Filter (AEKF).....	21
3.8 Randomized Analytical Solution as True Value	24
3.9 Examination of the Prediction Effectiveness	25
CHAPTER 4 Results and Discussion	27
4.1 Description of Simulation Parameters.....	27
4.2 Simulation Output of Numerical Model.....	27
4.3 Simulation Output of Extended Kalman Filter	31
4.4 Simulation Output of Adaptive Extended Kalman Filter	34

4.5 Analysis of the Prediction Models Effectiveness.....	42
4.6 Stability and Convergence Analysis of the Prediction Models.....	44
4.7 Process Noise Adjustment.....	46
4.8 Observation Noise Adjustment	48
CHAPTER 5 Conclusion and Future Research	52
References.....	56

List of Figures

Figure 3.1. Schematic representation of the Innovation Covariance and Gain Correction (ICS-GC) Adaptive Extended Scheme.	24
Figure 4.1. Comparison of numerical results and true value at time step 10.....	28
Figure 4.2. Comparison of numerical results and true value at time step 30.....	29
Figure 4.3. Comparison of numerical results and true value at time step 50.....	30
Figure 4.4. Comparison of EKF results and true value at time step 10.	32
Figure 4.5. Comparison of EKF results and true value at time step 30.	33
Figure 4.6. Comparison of EKF results and true value at time step 50.	34
Figure 4.7. Comparison of AEKF results and true value at time step 10.	35
Figure 4.8. Comparison of AEKF results and true value at time step 30.	36
Figure 4.9. Comparison of AEKF results and true value at time step 50.	37
Figure 4.10. Comparison of contaminant concentration prediction of BTCS, EKF, AEKF and True value at time step 10.....	39
Figure 4.11. Comparison of contaminant concentration prediction of BTCS, EKF, AEKF and True value at time step 30.....	40
Figure 4.12. Comparison of contaminant concentration prediction of BTCS, EKF, AEKF and True value at time step 50.....	41
Figure 4.13. Root Mean Square Error (RMSE) profile for BTCS, EKF and AEKF.....	43
Figure 4.14. Fifteen runs of RMSE profile for BTCS	44
Figure 4.15. Fifteen runs of RMSE profile for EKF.....	45
Figure 4.16. Fifteen runs of RMSE profile for AEKF.....	46

Figure 4.17. RMSE profile of AEKF for different process noise standard deviation (PNSD) values.	47
Figure 4.18. RMSE profile of AEKF for different observation noise standard deviation (ONSD) values	49
Figure 4.19. Comparison of AEKF performance with different window sizes.	50

List of Symbols

AEKF	Adaptive Extended Kalman Filter
EKF	Extended Kalman Filter
BTCS	Backward Time Central Space
ICS-GC	Innovation Covariance Scaling and Gain Correction
KF	Kalman Filter
A	State Transition Matrix (STM)
b	Aquifer thickness
C	Concentration of contaminant
C_0	Initial contaminant concentration
C_t	Predicted innovation covariance
\bar{C}_t	Estimated true innovation covariance
d_t	Innovation sequence at time step t
D_x, D_y	Dispersion coefficients in x and y directions respectively
H	Observation data pattern matrix
I	Identity matrix
K_t	Optimal Kalman gain matrix at time step t
\bar{K}_t	Corrected optimal Kalman gain matrix at time step t
k	First-order decay rate
M	Moving average window size
M_0	Initial contaminant mass input
m	Dimension of observation vector
n	Number of nodes in model domain

o_t	Observation noise vector at time t
p_t	Model system error or process noise vector at time step t
P_t	Optimal estimate error covariance matrix at time step t
\bar{P}_t	True optimal estimate error covariance matrix at time step t
Q_t	Model system error covariance matrix at time step t
R_t	Observation error covariance matrix at time step t
R	Retardation factor
RMSE (t)	Root-Mean-Squared-Error at time step t
Δt	Time step
V	Linear pore liquid velocity
x, y	Cartesian coordinates
x_t	Vector of contaminant concentration at time step t
x_t^T	True optimal contaminant concentration at time step t
$\Delta x, \Delta y$	Space interval along x and y directions respectively
z_t	Observations at time step t
α_t	Adaptive factor at time step t
λ_t	Forgetting factor at time step t
η	Porosity of porous medium
Ω	Boundary of studied area

Abstract

Pollution of groundwater can be harmful to the environment. The use of subsurface contaminant transport models, combined with stochastic data assimilation schemes, can give on-target predictions of contaminant transport to enhance the reliability of risk assessment in the area of environmental remediation. Observation data are required to guide the deterministic system model to assimilate the true state of the contaminant. Modeling the behavior of contaminant in groundwater is imperative in predicting the fate of the pollutant, in risk assessment, and as a preceding step of the remission process. In this study a two-dimensional transport model with advection and dispersion is used as the deterministic model of contaminant transport in the subsurface. An Adaptive Extended Kalman filter (AEKF) is constructed as a stochastic data assimilation scheme to meliorate the prediction of the contaminant concentration. Simulation results are shown to compare the performance of the numerical, the Extended Kalman filter and the AEKF. The effectiveness of the AEKF is determined by using a root mean square error (RMSE) of pollutant concentrations in contaminant transport modeling.

The results of the models indicate that, at the end of the simulation, the introduction of the Extended Kalman filter improved the deterministic model prediction by reducing the model error from 28 mg/L to 18 mg/L, thus improving the prediction accuracy by approximately 35.7%. The AEKF was successful in reducing the errors in the Extended Kalman filter prediction from 18 mg/L to 11 mg/L hence ameliorating prediction accuracy by approximately 38.9%. In general, the implementation of the AEKF was successful in improving the prediction accuracy of the deterministic model by about 60.7% which shows a substantial improvement in the prediction of the contaminant concentration in the subsurface environment.

CHAPTER 1

Introduction

The groundwater resource needs protection because of its utility to humans, the important role it plays in hydrological processes such as base-flow and also its susceptibility to pollutants. Some communities and cities in the United State of America depend solely on groundwater for water supply. Groundwater accounts for an estimated 20% of the total water usage in the United States and approximately 53% of the population rely on groundwater as a source of drinking water (NGWA and USGS, 2003).

Groundwater contamination occurs when man-made products such as gasoline, oil, road salts and chemicals get into the groundwater and cause it to become unsafe and unfit for human use. Some of the major sources of these products, called contaminants, are storage tanks, septic systems, hazardous waste sites, landfills, and the widespread use of road salts, fertilizers, pesticides and other chemicals. According to the United States Environmental Protection Agency (USEPA), about 15-20% of the over 1.8 million underground storage tanks containing petroleum products and other hazardous chemicals are either leaking or are expected to leak in the future (Chen et al., 1996). There are estimated to be over 10 million storage tanks buried in the United States and over time the tanks can corrode, crack and develop leaks. If the contaminants leak out and get into the groundwater, serious contamination can occur.

The Kalman filter is essentially a set of mathematical equations that implement a predictor-corrector type estimator that is optimal in the sense that it minimizes the estimated error covariance, when some presumed conditions are met. The simplicity of implementation and of the underlying mathematics has made the Kalman filter a popular tool for data assimilation problems. Because of its robustness, the filter has been applied to a wide range of problems often

regardless of the original assumptions. Besides the fact that the model should be linear, the central assumption that makes the Kalman filter a best linear unbiased estimator is that both model and observation errors are zero-mean and uncorrelated in time. The Kalman filter is the most commonly used state estimator in the target tracking problem, and its performance has been almost error free in situations where the target dynamics follow the model to a large extent (Welch and Bishop, 2006). The Kalman filter (KF) is a data assimilation technique that is able to process data recursively to generate optimum estimates of the state. The KF can be used for past, present and future state estimates (Welch and Bishop, 2006). Kalman filters are the best option to be used at the receiving end of the system.

A distinctive feature of the Kalman filter is to describe the mathematical formulation in terms of state-space concepts. Its solution is recursive, each updated estimate of the state is computed from the previous estimate and for new input data only the previous estimate is required to be stored (Khan and Khaled, 2010). But for situations where the target is actively maneuvering, i.e. doesn't follow the system model for most of the time, the Kalman filter has faltered in the estimation of states. Many advances in the Kalman Filter like the Neural Extended Kalman filter (Kathleen and Stephen, 2006); non-linear, non-Gaussian Kalman Filter and Hybrid Kalman Filters have been employed for tracking maneuvering targets. These filters, impressive as they are in their performance, are computationally complex and their correction capabilities can be redundant in cases where there is little or no measurement noise.

In evaluating the expected behavior of systems for contamination remediation, and in predicting the future accumulation of contaminant migration, a subsurface contaminant transport model plays a significant role in explaining how a plume of contamination develops.

In this study, an Adaptive Extended Kalman filter (AEKF) scheme is constructed by regulating the system error covariance and the optimal Kalman gain in order to reduce the effect of errors in the process and observation noise statistics during filter operation. The performance of the AEKF is compared with the numerical model and the Extended Kalman filter (EKF) in relation to the true field simulation. The effectiveness of the AEKF, EKF and the numerical model are assessed using root mean square error. The AEKF scheme is expected to improve the stability and convergence performance of the filter. The simulation is executed using a two-dimensional subsurface contaminant transport model. The Subsurface environment is considered to be heterogeneous; therefore, there are uncertainties in hydraulic parameters and the prediction model. Better prediction of subsurface contaminant transport will largely depend on the reliability of the parameter and the model used (Chang and Li, 2006).

The objectives for this research are to:

- (1) To improve the prediction of contaminant plume using Adaptive Extended Kalman filter and Extended Kalman Filter in a subsurface environment
- (2) To examine the performance of the Extended Kalman Filter and Adaptive Extended Kalman filter

CHAPTER 2

Literature Review

Information on the movement and behavior of contaminants in the subsurface at polluted location is necessary to comprehend the nature of the existing problem and the current or potential public health or ecological risks in order to put into place site-specific cleanup goals that are viable and to design a remediation program that is affordable, reliable and likely to achieve the cleanup goals. Knowledge of groundwater contaminant is required to avoid pumping contaminated water for human consumption.

The rate of change of dissolved solute with flowing groundwater is known as advection (Gorelick et. al., 1993). The amount of contaminant concentration transported is a function of time. Advection transport contaminants at different rates in each layer. Contaminant moves from an area of higher concentration towards an area where the concentration is less by a process called diffusion (Fetter, 1993). Diffusion can also take place when contaminant concentration in one stratum is greater than an adjacent stratum on condition that the adjacent stratum has the required porosity. Freeze and Cherry (1979) discussed retardation as the ratio between the velocity of the transporting fluid and that of the solute. Retardation is usually expressed as a number between one and infinity without units. First order decay rate is used in the two-dimensional transport model.

Hesham et al. (2009) developed a conceptual model to account for the different physiochemical and biological processes, reaction kinetics, and different transport mechanisms of the combined system (contaminant–colloids–bacteria). The presence of colloids affects contaminant transport in aquifers either by facilitation if the colloidal particles have smaller retardation factor than that of the contaminant or by retardation if they have a larger retardation

factor. Knowledge about the transport and fate of bacteria and viruses in porous media is essential for developing bioremediation strategies of contaminated sites (Rogers and Logan, 2000). It is expected that the model is capable of simulating contaminant transport in the presence of colloids and bacteria. Colloids and bacteria (microorganisms) naturally exist in groundwater aquifers and can significantly impact contaminant migration rates.

In another study, Park and Zhan (2001) investigated analytical solutions of contaminant transport from finite one, two, and three-dimensional sources in a finite-thickness aquifer. Their paper provides analytical solutions of contaminant transport from one, two, and three dimensional finite sources in a finite-thickness aquifer using Green's function method. A graphically integrated MatLab script is developed to calculate the temporal integrations in the analytical solutions and obtain the final solutions of concentration. Contaminant transport in the subsurface has been one of the most important research topics in the hydrological sciences and engineering in the last four decades (Bear, 1972; Gelhar, 1993; Domenico and Schwartz, 1998; Fetter, 1999).

Although many transport problems must be solved numerically, analytical solutions are still pursued by many scientists because they can provide better physical insights into the problems. Analytical solutions are usually derived from the basic physical principles and free from numerical dispersions and other truncation errors that often occurred in numerical simulations (Zheng and Bennett, 1995). Dispersion coefficients are assumed to be constants at all scales rather than scale-dependent variables as described (Gelhar, 1993).

Lin et al. (2010) developed a simplified numerical model of groundwater and solute transport. The simplified numerical model of 3-d groundwater and solute transport was used at large scale area. The validity of the developed 3-D groundwater model is tested with the typical

pumping and backwater scenarios. The solute transport module is tested against computing results using the MT3DMS Based on a representative 3-D pollution case. A variety of analytical solutions derived from the basic physical principles have been presented which are mostly suitable under special boundary conditions. The capability and high efficiency to predict non-stationary situations of free groundwater surface and solute plume in regional scale problem is quantitatively investigated. It is shown that the proposed model is computationally effective. When predicting solute plume, high computation efficiency is achieved with the simplified model.

A three-dimensional numerical model for groundwater flow and heat transport is used to analyze the heat exchange in the ground (Lee, 2011). The influence of pressure gradient, which determines the velocity of regional groundwater flow, is most substantial. At present, the use of computer modeling constitutes an integral part in the prediction and evaluation of geothermal performance (Breger et al., 1996). The effect of pressure-specified boundary conditions was first evaluated. To evaluate the sensitivity of groundwater flow to the performance of the Standing Column Well (SCW) system is essential to provide an optimized configuration and operation schedule for boreholes on the site.

Chemicals entering the subsurface can spread downward and laterally, contaminating a large volume of soil, and may reach the groundwater or degrade pipe and utility lines. A major concern is how and to what extent these contaminants affect the drinking water supply. Mathematical and numerical modeling of the fate and transport of chemical species in the subsurface has become a critical area of research over the past several years. Spills, improper disposal, and leaking storage tanks are but a few of the ways that chemicals infiltrate the subsurface.

Computational algorithms have been formulated and implemented on distributed memory computer platforms for modeling multiphase flow and reactive transport problems in porous media. There are several remediation strategies being studied, depending on the type and location of the contaminants and whether they are in the groundwater or trapped in partially saturated soils. Generation models of flow through porous media with general aqueous reactions (Walsh et al., 1984) showed the importance of developing a theoretical understanding of the dynamics of concentration fronts (Bryant et al., 1987, Dria et al., 1987).

A mathematical formulation and some numerical approximation techniques are described for a system of coupled partial differential and algebraic equations describing multiphase flow, transport and interactions of chemical species in the subsurface (Todd et al., 1995). The ability to account simultaneously for fluid flow and chemical reactions is essential for evaluating many groundwater contamination problems.

Mathematical models have been recognized as the most effective tool for explaining how a plume of contaminant evolves. Subsurface contaminant transport models can describe the spatial and temporal distribution of contaminant as well as their movement to potential receptor points (Tam and Beyer, 2002). In order to design cost-effective remediation systems for contaminated sites, a detailed understanding of the flow and transport of contaminants is required. Over the past few decades, various efforts have been made to understand the fate and transport of pollutants in the subsurface. However, a number of factors including the difficulty in determining the field coefficient of dispersion and velocity of water as well as the challenges involved in the quantification of chemical reaction terms have limited the routine use of such models. Regional size models which neglect the effects of dispersion have also had limited success due to the scarcity and poor quality of field data.

Cheng and Yeh (1998) addressed the issue of development and demonstrative application of a 3-D numerical model of subsurface flow, heat transfer, and reactive chemical transport. The flow equation is discretized by the Galerkin finite element method. Modeling of chemical transport in subsurface systems incorporating chemical equilibrium and kinetics-controlled reactions along the flow path has become one of the major task facing hydrogeologists and geochemists today. The increasing public concerns about ground water contamination directed the attention of ground water hydrologists to the study of the transport of chemicals in subsurface systems in the field of ground water hydrology. Tompson and Jackson (1996) also pointed out how chemical heterogeneity can affect the overall mobility and species configuration within contaminant mixture in the subsurface.

Gerald (2011) applied the finite difference method to a partial differential equation. The partial differential equation is replaced with a discrete approximation in the numerical solution. The backward time, centered space (BTCS) was formulated and applied to one-dimensional heat equation. Complete MatLab code for the scheme was presented which was working. The finding in the studies shows that the backward time, centered space scheme is just as accurate as the forward time, centered space (FTCS) scheme.

The Kalman filter is a data assimilation technique that is able to process data recursively to generate optimum estimates of the state. Chang and Jin (2005) improved the efficiency of a contaminant transport models by using Kalman filter with regional noise. The Kalman filter can be used for past, present and even future state estimates (Welch and Bishop, 2006). The effectiveness and efficiency of the Kalman filter is due to its ability to handle dynamic and stochastic processes, providing optimal solutions for linear systems (Chang and Jin, 2005). The

contaminant state distribution and its corresponding noise fields are assumed to be Gaussian in the operation of the Kalman filter.

The data assimilation scheme of the Kalman filter is particularly effective when both system and observation models are linear (Welch and Bishop, 1995). The implementation of Kalman filter requires that the complete a priori statistical knowledge of the process noise and measurement noise are available. Most applications of Kalman filter in hydrology have been done based on Gaussian noise assumptions. The Kalman filter data assimilation scheme is particularly effective when both system and observation models are linear (Welch and Bishop, 2006). Chang and Latif (2007) applied Kalman filter as well as Particle filter in a one dimensional leachate transport in subsurface. The Kalman filter has been used in subsurface contaminant transport and groundwater flow modeling for last three decades (Chang and Jin, 2005; Eppstein and Dougherty, 1996; Geer, 1982; Zou and Parr, 1995).

The Extended Kalman filter is the nonlinear adaptation of the Kalman filter which gets into a linear form about an estimate of the current mean and covariance. Chang and Latif (2010) applied Extended Kalman filter to improve the accuracy of a subsurface contaminant transport model. The effectiveness of Extended Kalman filter was tested using the root mean square error (RMSE). The Extended Kalman filter gave a favorable prediction than the numerical and the Kalman filter.

In another study, Zhang and Zhao (2011) investigated the performance comparison and analysis of Extended Kalman filters for global positioning system (GPS) / dead reckoning (DR) navigation. Several nonlinear filtering algorithms based on the dead reckoning and the global positioning was proposed. A central problem in many engineering and contemporary applications in science lies in developing techniques for real-time statistical estimation of a state

of a complex natural system based on partial observations and an imperfect model. Recently, Stochastic Parameterization Extended Kalman Filter was used as benchmark for propagating the mean and covariance of the augmented forecast model (Branicki et al., 2012). The sole reasoning of the filtering technic is to obtain, recursively in time, favorable estimates of the state of a stochastic dynamic system based on noisy partial observations (Budhiraja et al., 2007). Given a set of partial and noisy observations (measurements) of the states, the problem of interest is to estimate the states of an engineering dynamical system. The Kalman filter is exact and widely used for state estimations of linear dynamical systems while system models in most identification problems of practical interest are non-linear (Saha and Roy, 2009).

Becerra et al. (2001) applied the Extended Kalman filter to systems described by nonlinear differential-algebraic equations. The Extended Kalman filter uses local linearization to extend the scope of the Kalman filter to systems described by nonlinear ordinary differential equations (Maybeck, 1982). Gerald and Peter (2006) proposed the used of frequency-domain Adaptive Kalman filter. Kalman filter for adaptive echo cancelation was evaluated (Meissner et al., 1980).

Han et al. (2009) presented an Adaptive Extended Kalman filter method to estimate the state-of-charge. The Adaptive Extended Kalman filter reduced the state-of-charge estimation error when working with the unknown process and measurement noise covariance values. The estimation errors were reduced by using the Adaptive Kalman filter, which modifies the covariance adaptively. Identification and quantification of method of overlapped peaks in liquid chromatography with UV diode array detection was reported using an Adaptive Kalman filter (Chen and Rutan, 1996).

Also, an Adaptive Extended Kalman filter was developed and investigated for a transient heat transfer problem (Myers et al., 2012). It was observed that adjustments made to either the measurement covariance or the state model covariance affects the convergence behavior of the Kalman filter. However, the state model covariance is entirely not known and is obtained through trial and error. In their work, the Adaptive Extended Kalman filter constructed produces faster and smoother convergence than the non-adaptive form of the Extended Kalman filter.

In another study, a data fusion based on Adaptive Extended Kalman filter algorithm was used to centralized and decentralized process and sensor fault monitoring (Salahshoor et al., 2008). Constant diagonal matrices for both the process and measurement covariance assumption approach were used in the classical Extended Kalman filter implementation. Adaptive Extended Kalman filter and probabilistic neural network (PNN) were combined in power distribution feeders in an intelligent approach for high impedance fault (HIF) detection (Samantaray et al., 2009). An Extended Kalman filter and Kalman filter are proposed and used subsequently to fuse a data from inertial navigation system (INS) sensors and to integrate them with a GPS data (Loebis et al., 2004).

Moreover, to enhance the robustness of the Kalman filter algorithm with respect to modeling error and measurement noise an adaptive version of the Extended Kalman filter is proposed (Lippiello et al., 2007). In the literature various algorithm of Adaptive Extended Kalman filter have been proposed, where the problem of the real-time adaptation of the statistical parameters of the covariance matrices of the state and observation noise in different applications are addressed (Girgis and Peterson, 1990). The performance of the Extended Kalman filter versus the Adaptive Extended Kalman filter are compared using different object flights as well as

to appreciate the effects of the update laws for the state and observation noise covariance matrices separately are presented in a number of case studies.

In this research, the numerical solution was discretized using backward in time and centered in space (BTCS). The effectiveness and the performance of the proposed AEKF and EKF algorithm have been experimentally tested using root mean square error.

CHAPTER 3

Methodology

3.1 Deterministic Model

A two-dimensional subsurface advection-dispersion model for the transport of contaminant in the horizontal plane (x-y) and advection in the x direction was used to examine the accuracy and effectiveness of the numerical, the Extended Kalman filter and the Adaptive Extended Kalman filter results relative to the analytical solution that has been randomized (reference true value). The advection-dispersion equation for a two dimensional transport in the x-y plane is described by the following partial differential equation

$$\frac{\partial C}{\partial t} = \frac{D_x}{R} \left(\frac{\partial^2 C}{\partial x^2} \right) + \frac{D_y}{R} \left(\frac{\partial^2 C}{\partial y^2} \right) - \frac{V}{R} \left(\frac{\partial C}{\partial x} \right) - \frac{k}{R} C \quad (1)$$

C = concentration of contaminant in the solute phase (mg/L)

t = time (day)

D_x = dispersion coefficients in x directions (m^2/d)

D_y = dispersion coefficients in y directions (m^2/d)

V = linear velocity in the x-direction (m/d)

R = retardation factor

k = first-order decay rate (1/day)

The boundary condition of the two-dimensional mass transport with an instantaneous point source is expressed as

$$C(x, y, t)|_{t=0} = C_0(x_i, y_i) \quad (2)$$

$$C(x, y, t)|_{t=\Omega} = 0 \quad (3)$$

Where (x_i, y_i) is the initial co-ordinate that the pulse input occurred and Ω is a representation of a square boundary.

3.2 Numerical Solution Approach

In order to express the deterministic model in a more convenient form for the implementation of the data assimilation schemes, a Backward-Time and Central-Space (BTCS) differencing scheme was developed to solve the two-dimensional transport model numerically. In this research, the Backward in time and centered in space approach is used to generate one set of results and later used in the system equation in the Kalman filtering process. Since most contaminant undergoes a decay process, a first order decay factor k is assumed and introduced into the numerical scheme. The deterministic model is discretized by substituting the finite difference approximations into the two-dimensional subsurface equation. The general BTCS scheme forms of the numerical model are given as:

$$\frac{\partial C}{\partial t} \approx \frac{C(x, y, t) - C(x, y, t-1)}{\Delta t} \quad (4)$$

$$\frac{\partial C}{\partial x} \approx \frac{C(x+1, y, t-1) - C(x-1, y, t-1)}{2\Delta x} \quad (5)$$

$$\frac{\partial^2 C}{\partial x^2} \approx \frac{C(x+1, y, t-1) - 2C(x, y, t-1) + C(x-1, y, t-1)}{\Delta x^2} \quad (6)$$

$$\frac{\partial^2 C}{\partial y^2} \approx \frac{C(x, y+1, t-1) - 2C(x, y, t-1) + C(x, y-1, t-1)}{\Delta y^2} \quad (7)$$

$$kC \approx kC(x, y, t-1) \quad (8)$$

The resulting iteration scheme after discretizing the concentration in the model domain is expressed as

$$C(t, x) \approx \Psi_1 C(x-1, y, t-1) + \Psi_2 C(x, y, t-1) + \Psi_3 C(x+1, y, t-1) + \Psi_4 C(x, y-1, t-1) + \Psi_5 C(x, y+1, t-1) \quad (9)$$

Where

$$\Psi_1 = \frac{D_x \Delta t}{R \Delta x^2} + \frac{V \Delta t}{2R \Delta x}$$

$$\Psi_2 = 1 - \frac{2D_x \Delta t}{R \Delta x^2} - \frac{2D_y \Delta t}{R \Delta y^2}$$

$$\Psi_3 = \frac{D_x \Delta t}{R \Delta x^2} - \frac{V \Delta t}{2R \Delta x}$$

$$\Psi_4 = \frac{D_y \Delta t}{R \Delta y^2}$$

$$\Psi_5 = \frac{D_y \Delta t}{R \Delta y^2}$$

The convergence and stability criteria for the scheme are given as

$$\Delta x < \frac{2D_x}{V} \quad (10)$$

and

$$\Delta t < \frac{1}{\left(\frac{2\Delta y D_x}{\Delta x^2 R} \right)} \quad (11)$$

Equation 9 can be rewritten in a state-space form as

$$\mathbf{x}_t = \mathbf{A} \mathbf{x}_{t-1} \quad (12)$$

Where

\mathbf{x}_t = the vector of contaminant concentration at all nodes at time, t

\mathbf{x}_{t-1} = the vector of contaminant concentration at all nodes at time, t-1

A = the State Transition Matrix (STM) containing the parameters for the model which advances the current state to the next time step.

3.3 Process Equation

A random Gaussian noise is introduced into the numerical scheme to simulate the contaminant transport because of the stochastic and heterogeneous nature of the subsurface environment. Transport processes can be simulated by stochastic data assimilation schemes with uncertain sources and inaccurate transport parameters by introducing a random noise term in the deterministic dynamics (Saad, 2007).

$$\mathbf{x}_t = \mathbf{A}\mathbf{x}_{t-1} + \mathbf{p}_t, t = 0, 1, 2, 3 \dots \quad (13)$$

Where

\mathbf{x}_t = vector of contaminant concentration at all nodes at time, t ;

\mathbf{x}_{t-1} = vector of contaminant concentration at all nodes at time, $t-1$

\mathbf{A} = State Transition Matrix (STM) that runs till the last time step

\mathbf{p}_t = model system error or process noise.

The system model error, \mathbf{p}_t is assumed to have zero mean and covariance matrix, \mathbf{Q}_t . The model system error is the difference between the optimal estimate of the true state and the model prediction.

3.4 Measurement Equation

Since field data are difficult and costly to acquire, the analytical solution with a 5% Gaussian noise added to it was adopted as the true value in this study. Random Gaussian noise was added to the true value to obtain observation data or measurement for all time steps, and used in the filtering process. The observation error introduced takes care of instrumental errors, human errors and the randomized nature of a practical field data of contaminant concentrations.

The equation governing the observation data for the entire domain in this study is given as

$$Z_t = HX_t^T + O_t \quad (14)$$

Where

Z_t = state vector for observed vales for all nodes at time step t

H = measurement sensitivity matrix

X_t^T = the transpose of the true optimal estimate of the state

O_t = vector of the observation error

The observation noise, O_t is assumed to have zero mean and covariance matrix R_t . H is constructed as an identity matrix with n being the number of nodes in the model domain, in this study the number of nodes were chosen to be 625.

3.5 Kalman Filter Algorithm

In 1960, Rudolf Kalman developed the Kalman filter, which is an efficient recursive filter that estimates the states of a dynamic system from a series of incomplete and noisy measurements. The filter is considered to be a very powerful tool since it supports estimation of past, present and even future states even when the precise nature of the modeled system is unknown (Welch and Bishop, 1995). The Kalman filter equations fall into two groups; time update or predictor equations and measurement update equations or corrector equations.

Prediction Stage:

$$\mathbf{x}_t(-) = \mathbf{A}\mathbf{x}_{t-1} + \mathbf{p}_t \quad (15)$$

$$\mathbf{P}_t(-) = \mathbf{A}\mathbf{P}_{t-1}\mathbf{A}^T + \mathbf{Q}_t \quad (16)$$

Update Stage:

$$\mathbf{K}_t = \mathbf{P}_t(-)\mathbf{H}^T(\mathbf{H}\mathbf{P}_t(-)\mathbf{H}^T + \mathbf{R}_t)^{-1} \quad (17)$$

$$\mathbf{x}_t(+) = \mathbf{x}_t(-) + \mathbf{K}_t[\mathbf{z}_t - \mathbf{H}\mathbf{x}_t(-)] \quad (18)$$

$$\mathbf{P}_t(+)= (\mathbf{I} - \mathbf{K}_t \mathbf{H}) \mathbf{P}_t(-) \quad (19)$$

Where

$x_t(-)$ = the estimated state vector before the Kalman filter adjustment with covariance $P_t(-)$

$x_t(+)$ = the estimated state vector after the KF adjustment with covariance $P_t(+)$

K_t = the optimal Kalman gain matrix which minimizes the optimal estimate error covariance matrix, P_t .

\mathbf{I} = an identity matrix.

$P_{t-1}(-)$ and $x_{t-1}(-)$ are initially specified to start the Kalman Filter data assimilation process.

3.6 Extended Kalman Filter

The Extended Kalman filter (EKF) is the nonlinear version of the Kalman filter which linearizes about an estimate of the current mean and covariance. It provides a consistent first-order approximation to the optimal estimate of the state and of the time-dependent model uncertainties, both when data are available and when they are not (Kao et al., 2003). A Kalman Filter that linearizes about the current mean and covariance is referred to as an Extended Kalman filter (Welch and Bishop, 1995). The two nonlinear dynamical state –space models are

$$x_{t+1} = A(t, x_t) + p_t \quad (20)$$

$$z_t = h(t, x_t) + o_t \quad (21)$$

The functional $A(\mathbf{t}, \mathbf{x}_t)$ and $h(\mathbf{t}, \mathbf{x}_t)$ represent nonlinear transition matrix function and nonlinear measurement matrix that are time-variant respectively.

The nonlinear matrices are transformed into partial derivatives given as;

$$F_{t+1} = \frac{\partial A(t, x_t)}{\partial x} \quad (22)$$

$$H_t = \frac{\partial h(t, x_t)}{\partial x} \quad (23)$$

Where, F_{t+1} and H_t are the Jacobian matrices for the state transition and the measurement respectively. Using the basic idea of Kalman Filtering, the transformed state transition and measurement matrix is then used which makes the filter to work in the extended form.

3.7 Adaptive Extended Kalman Filter (AEKF)

The Extended Kalman filter remains a popular choice that has been applied in various fields. However, the Extended Kalman filter is vulnerable to linearization errors, which can lead to poor performance or divergence (Guoquan and Stergios, 2008). Also, the Extended Kalman filter assumes a complete knowledge of the process and observation noise covariance matrices which may be estimated inaccurately and causes the filter to diverge (Hide et al. 2004).

Therefore, the uncertainties in the process and observation noise covariance are addressed by introducing the adaptive filtering technique into the Extended Kalman filter scheme.

An Adaptive Extended Kalman filter is envisioned where changes are made during each iteration to the state model covariance to improve convergence. It is expected that, the execution of an Adaptive Extended filter will help to reduce the effect of unaccounted errors in the process and observation noise covariances. The adaptive filtering technique which is based on the Innovation Covariance Scaling and Gain Correction (ICS-GC) addresses the effect of unaccounted errors in the process and observation models (Kim and Lee, 2006). The algorithm for the AEKF is given as

Prediction Stage:

$$\mathbf{x}_t(-) = \mathbf{A}\mathbf{x}_{t-1} + \mathbf{p}_t \quad (24)$$

$$\bar{\mathbf{P}}_t(-) = \alpha_t [\mathbf{A}\mathbf{P}_{t-1}\mathbf{A}^T + \mathbf{Q}_t] \quad (25)$$

Update Stage:

$$\bar{\mathbf{K}}_t = \bar{\mathbf{P}}_t(-)\mathbf{H}^T (\mathbf{H}\bar{\mathbf{P}}_t(-)\mathbf{H}^T + \lambda_t \mathbf{R}_t)^{-1} \quad (26)$$

$$\mathbf{x}_t(+) = \mathbf{x}_t(-) + \bar{\mathbf{K}}_t [\mathbf{z}_t - \mathbf{H}\mathbf{x}_t(-)] \quad (27)$$

$$\bar{\mathbf{P}}_t(+) = (\mathbf{I} - \bar{\mathbf{K}}_t \mathbf{H})\bar{\mathbf{P}}_t(-) \quad (28)$$

Where

$\mathbf{x}_t(-)$ = the estimated state before the AEKF adjustment with covariance $\mathbf{P}_t(-)$

$\mathbf{x}_t(+)$ = the estimated state after the AEKF adjustment with covariance $\mathbf{P}_t(+)$

$\bar{\mathbf{K}}_t$ = the optimal Kalman gain matrix which minimizes the optimal estimate error covariance matrix, \mathbf{P}_t .

\mathbf{I} = an identity matrix.

λ_t = Forgetting factor at time step t

α_t = Adaptive factor at time step t

$$\alpha_t = \max \left\{ 1, \frac{1}{m} \text{tr}(\bar{\mathbf{C}}_t \mathbf{C}_t^{-1}) \right\} \quad (29)$$

$$\bar{\mathbf{C}}_t = \frac{1}{M-1} \sum_{i=t-M+1}^t \mathbf{d}_i \mathbf{d}_i^T \quad (30)$$

$$\mathbf{d}_t = \mathbf{z}_t - \mathbf{H}\mathbf{x}_t(-) \quad (31)$$

$$\mathbf{C}_t = E[\mathbf{d}_t \mathbf{d}_t^T] = \mathbf{H}\bar{\mathbf{P}}_t(-)\mathbf{H}^T + \mathbf{R}_t \quad (32)$$

$$\bar{\mathbf{C}}_t = \mathbf{H}\bar{\mathbf{P}}_t(-)\mathbf{H}^T + \lambda_t \mathbf{R}_t \quad (33)$$

$$\bar{\mathbf{C}}_t = \alpha_t \mathbf{C}_t \quad (34)$$

$$E[\mathbf{d}_t \mathbf{d}_t^T] = \mathbf{H}\bar{\mathbf{P}}_t(-)\mathbf{H}^T + \lambda_t \mathbf{R}_t \quad (35)$$

$$\lambda_t = \frac{tr(\mathbf{d}_t \mathbf{d}_t^T) - tr(\mathbf{H} \bar{\mathbf{P}}_t(-) \mathbf{H}^T)}{tr(\mathbf{R}_t)} \quad (36)$$

Where \mathbf{d}_t is the innovation sequence which is the difference between the observation and the predicted state at a given time. $\bar{\mathbf{C}}_t$ is the estimated true innovation covariance, \mathbf{C}_t is the predicted innovation covariance is dimension of observation vector; M is the moving window size (Fathabadi et al., 2009), λ_t is called a forgetting factor and $\lambda_t > 1$, α_t is the adaptive factor and $\alpha_t > 1$ (Hu et al. 2003; Weidong et al. 2006). Equation (25) is the expression for the error covariance estimation for the AEKF. Equation (26) is the corrected optimal Kalman gain expression for the AEKF and Equation (33) is the estimated true innovation covariance (Hajiyev, 2007).

The above equations (24), (25), (26), (27) and (28) represent the adaptive system which has been created by the introduction of a corrected optimal Kalman gain and a true system covariance. The schematic representation of the ICS-GC Adaptive Extended filter scheme is shown in Figure 3.1. The figure gives an overview of the operation of the Adaptive Extended filter scheme. The Extended Kalman filter combines the observation and the system model to give an estimation, as the filtering proceeds the adaptive factor adjust the process noise covariance (Kim and Lee 2006) while the forgetting factor is estimated to adjust the observation noise covariance by correcting the Kalman gain (Hajiyev, 2007), after which the Adaptive Extended Kalman filter is expected to give an accurate prediction.

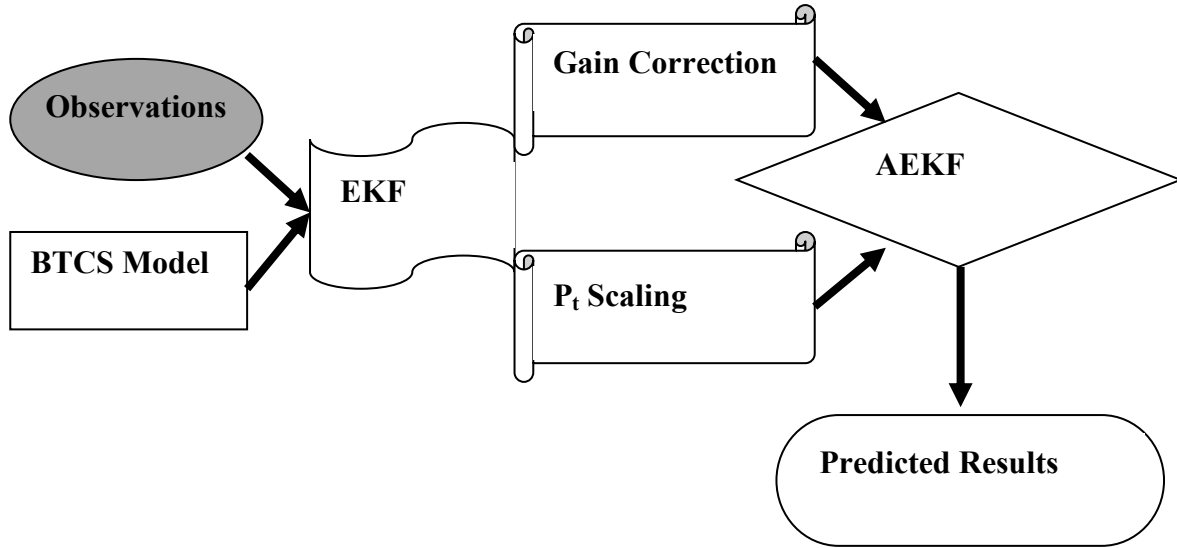


Figure 3.1. Schematic representation of the Innovation Covariance and Gain Correction (ICSGC) Adaptive Extended Scheme.

3.8 Randomized Analytical Solution as True Value

In order to implement the data assimilation schemes, observation information is required to guide the system model to project the optimal contaminant concentration. Various studies have simulated synthetic observation data by creating “true field” conditions (McLaughlin, 2002). The analytical solution which has been randomized governing the advection-dispersion partial differential equation is given by

$$C(x, y, t) = \frac{M_0}{4\pi b \eta t \sqrt{D_x D_y}} e^{\left(-\frac{(x-Vt/R)^2}{4D_x t/R} - \frac{y^2}{4D_y t/R} - kt \right)} + w_t \quad (37)$$

Where

C = concentration of contaminant in the solute phase (mg/L)

D_x = dispersion coefficients in x directions (m^2/d)

D_y = dispersion coefficients in y directions (m^2/d)

η = porosity of the medium

b = aquifer thickness (m)

R = retardation factor (dimensionless)

V = linear velocity in the x-direction (m/d)

k = the first-order contaminant decay rate (1/day)

M_0 = instantaneous mass input (g)

x = Cartesian coordinates (m) in the x direction

y = Cartesian coordinates (m) in the y direction

t = time (day)

$w_t = \{0, 5\%\}$

Equation (37) represents the variations in time and distance in concentration, depending on the initial mass of contaminant per unit area injected across the aquifer cross section during a spill at time $t = 0$. An observation was created by introducing an observation error of 2.5% into the true value.

3.9 Examination of the Prediction Effectiveness

The root mean square error (RMSE) was used as an indicator performance to measure the effectiveness of AEKF, EKF and numerical results. The model predictions are compared with a simulated true field to estimate the error parameter (RMSE). The RMSE indicates the degree of error in each result in relation to the true value. The RMSE is given as

$$RMSE(t) = \sqrt{\frac{1}{N-1} \sum [C^T(x, y, t) - C^P(x, y, t)]^2}$$

Where

RMSE (t) = Root Mean Square Error (mg/L) at time step, t.

N = Number of sampling nodes.

$C^P(x, y, t)$ = Predicted value of concentration at node (x, y) at time step, t .

C^T = Reference true value of concentration at node (x, y) at time step, t .

CHAPTER 4

Results and Discussion

4.1 Description of Simulation Parameters

The simulation was conducted using a 37.5 m by 37.5 m domain space with grid points of 625 on a two-dimensional plane. The grid intervals used in this study in the two dimensional plane in the x direction, Δx is 1.5 m and that of the y direction, Δy is also given as 1.5 m. The parameter values used in the subsurface to simulate the contaminant transport were acquired from Zou and Parr (1995). The dispersion coefficients, D_x in x directions and the dispersion coefficients, D_y , in y directions are 1.554 m²/d and 0.4662 m²/d, respectively. The time adopted for each time step, the thickness of the aquifer, and the porosity, η , in the analytical equation were taken as 0.2 day, 6.1 m and 0.3, respectively. The retardation factor, R , is assumed to be 1.2 while the linear velocity, V , is taken to be 1.5 m/d. To create a random noise condition, a standard deviation of 2.5% and 5% was brought to bear as the observation error and process error, respectively in the modeling process.

In practice, it is costly and labor intensive to construct observation wells at every point in the model domain, therefore, twelve sparse measurement data set was used to predict the simulation area of the 625 nodes. The initial concentration of contaminant injected into the grid point at coordinates (5, 10) in the 37.5 × 37.5 space domain was 10,000 mg/L and the instantaneous contaminant mass at the grid point is 1604g. Simulations were carried out by running MatLab codes for numerical, reference true, EKF and AEKF.

4.2 Simulation Output of Numerical Model

MatLab code is formulated based on the partial differential equation (advection-dispersion equation for a two dimensional transport) as indicated in Equation (1). The contour

profiles of the deterministic model (BTCS) are compared with the simulated true value which serves as true field value in this study. Figure 4.1, Figure 4.2 and Figure 4.3 shown below represent the contours of the contaminant plume by the deterministic model in comparison with the true value at time steps 10, 30 and 50, respectively. From Figure 4.1, Figure 4.2 and Figure 4.3, the prediction by the deterministic model distinctly departs slower than the true value which can be attributed to linear velocity used in estimation process, numerical errors, which are round off errors, truncation errors, instability to mention but few as indicated by Spitz and Moreno (1996).

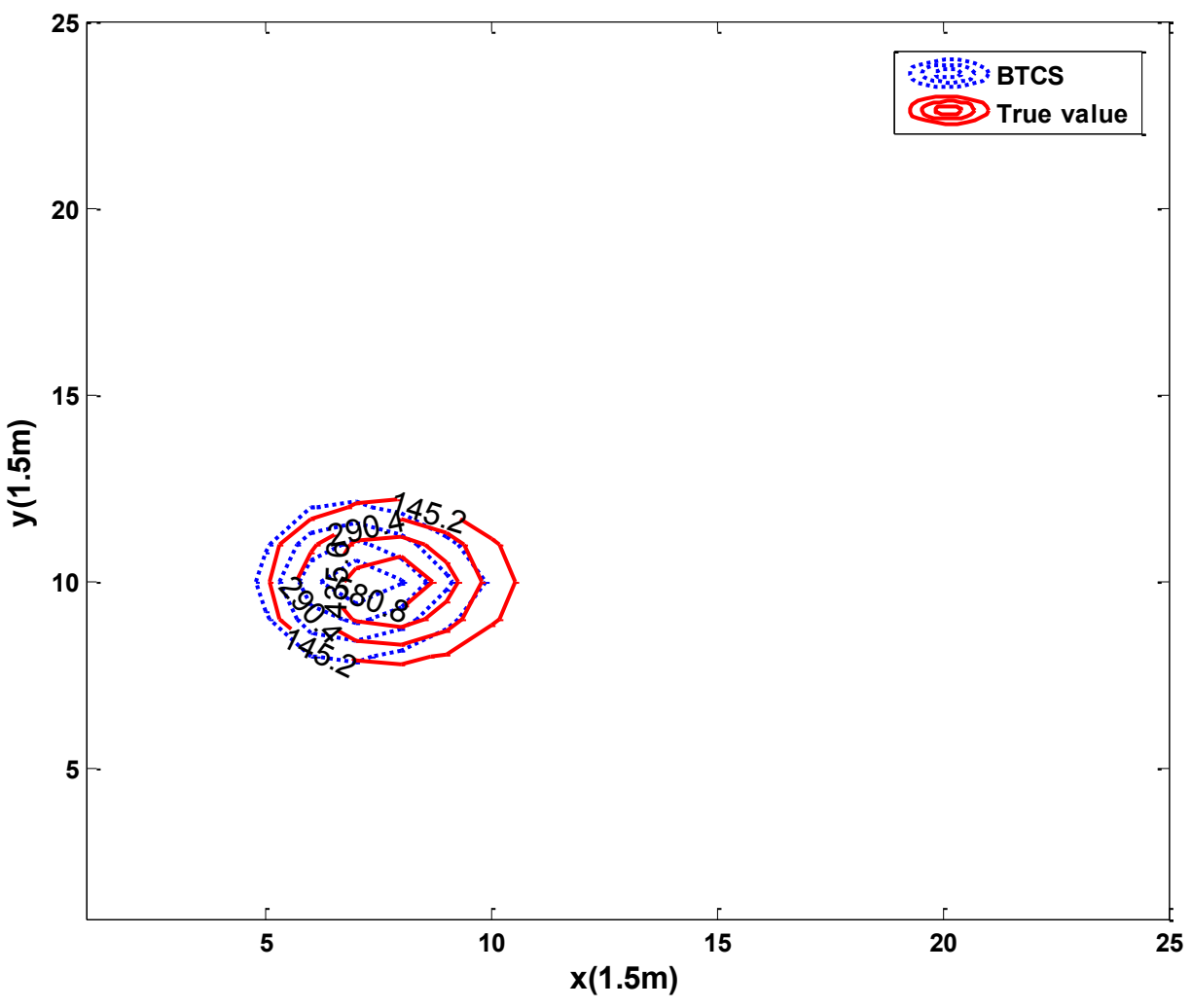


Figure 4.1. Comparison of numerical results and true value at time step 10.

The size of the contaminant plume keeps increasing as the time step increased for both the numerical results and the true value. From the results, the dispersion of the contaminant plume of the deterministic model is lesser. At time step 50 deviation of the deterministic model from the true value was visibly evident. The smallest and the highest concentration at time step 50 are approximately 24.8 mg/L and 99.2 mg/L, respectively which indicate that about 1% of the initial contaminant concentration remains at that time step.

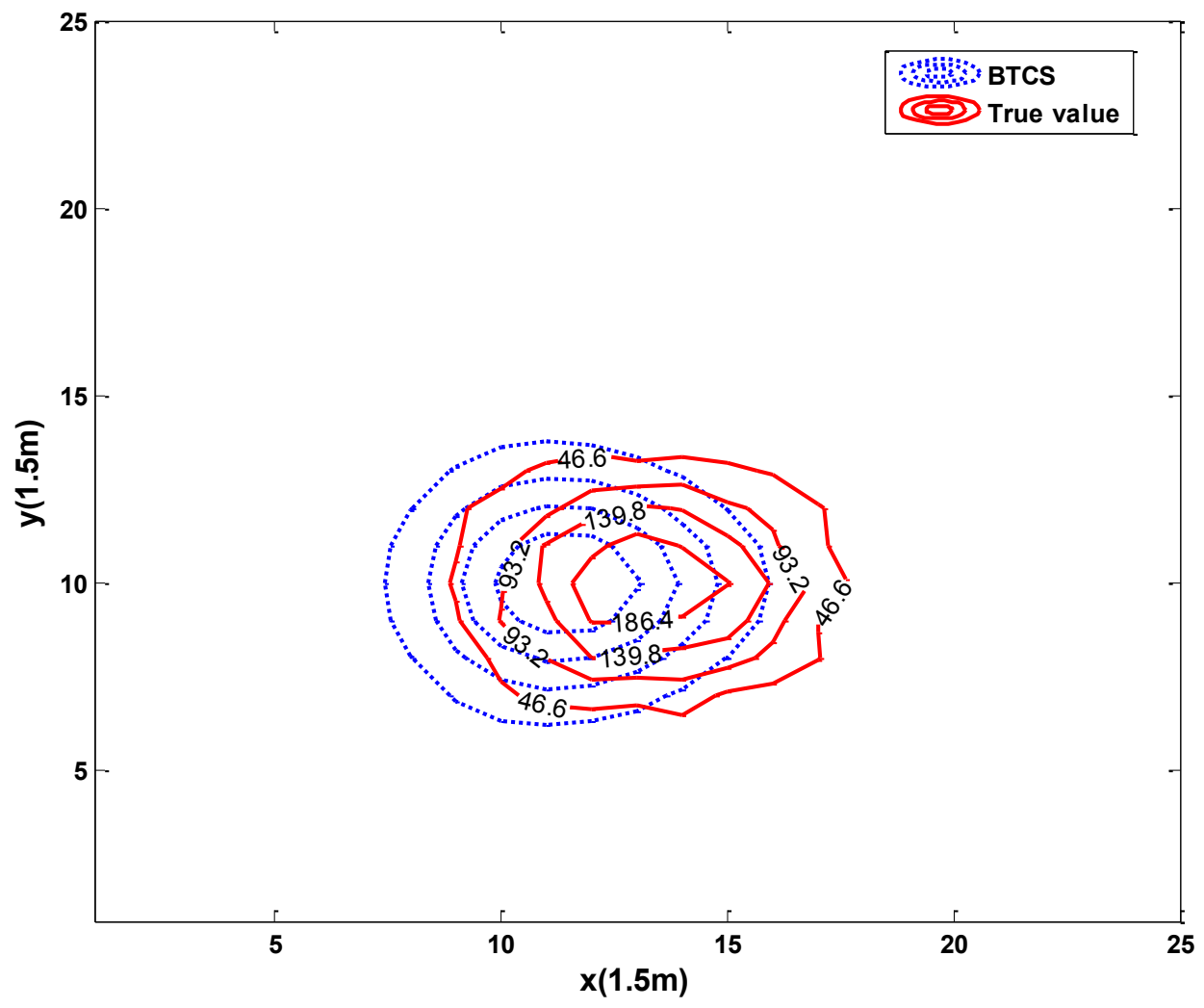


Figure 4.2. Comparison of numerical results and true value at time step 30.

It can be realized that as the contaminant plume migrate from its initial source the plume size keeps increasing whereas the concentration reduces because of such processes as dispersion, time rate release of contaminants, and distance of travel. The contaminant plume of the deterministic model has comparatively smooth shape as a result of the approximation made to it.

Many factors combine to determine the quality and usefulness of a model predication. Numerical methods involve approximations which introduce errors into the deterministic model thereby affecting the accuracy and precision of the prediction. The setting of stability and convergence criteria in the results generation is another form of error in the numerical approach.

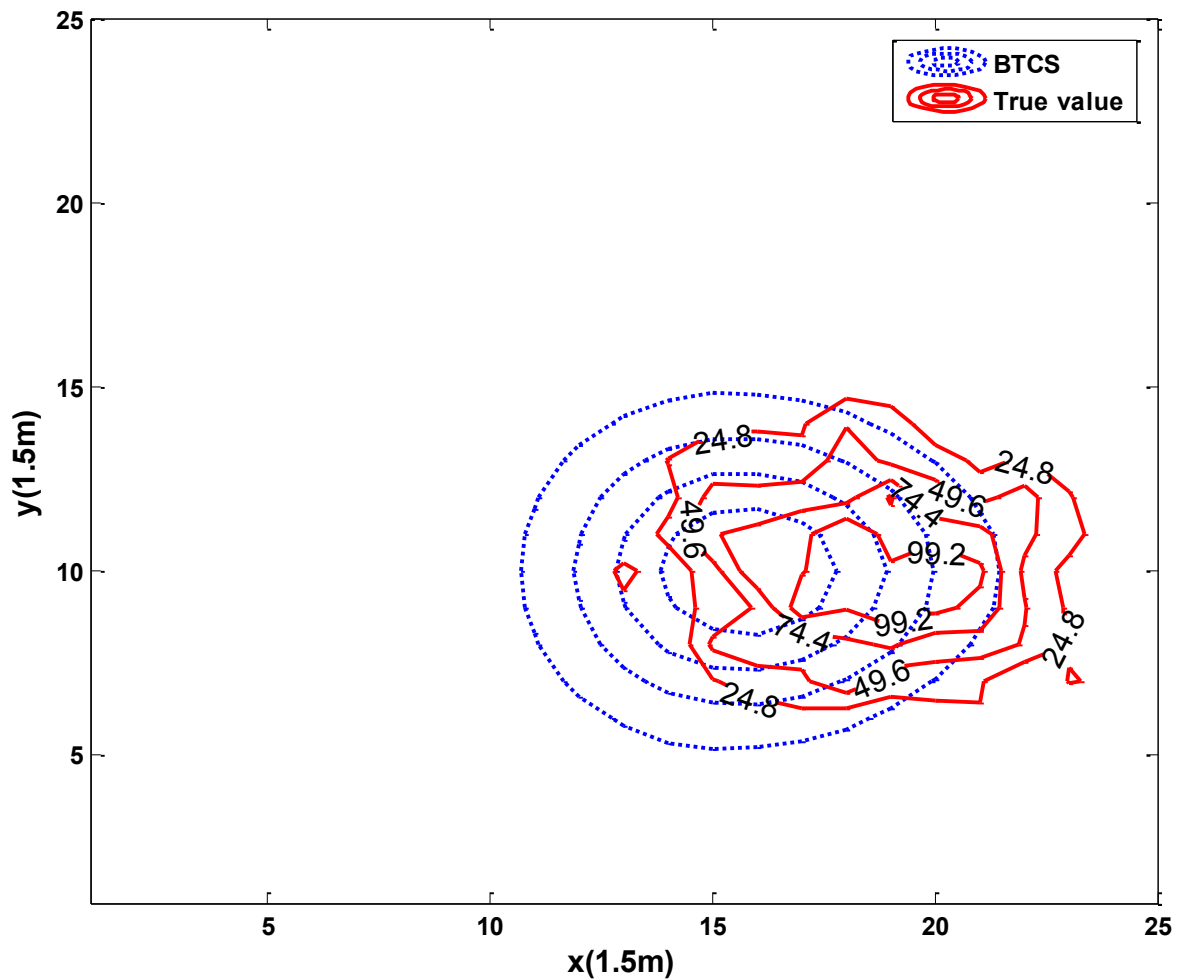


Figure 4.3. Comparison of numerical results and true value at time step 50.

Moreover, due to the heterogeneous nature of the subsurface, hydraulic parameters and initialization data acquired from the field may vary, as a result assumptions are made on the parameters and the model used in estimation which further introduce error into the numerical method. The numerical model is unable to simulate a true field condition accurately because it provides an approximate solution to the transport equation. Despite the fact that numerical model is useful in predicting the fate and transport of contaminants in groundwater, the complex nature of the subsurface environment makes it extremely difficult to give accurate prediction.

4.3 Simulation Output of Extended Kalman Filter

The Extended Kalman filter which is a nonlinear extension of the Kalman filter as proposed by Jazwinski (1970) is used in this study. The Extended Kalman filter is used in the two-dimensional transport model to predict the state of the contaminant plume in the subsurface. The Extended Kalman filter resolves the problem of nonlinear measurement functions by local linearization of those nonlinear functions by taking the partial derivatives of those functions. (Welch and Bishop, 1995). A Gaussian noise was injected into the system model during the implementation of the Extended Kalman filter to account for the variability in the hydraulic parameters since it is stochastic in nature. Chang and Latif (2010) applied the Extended Kalman filter to improve the accuracy of a subsurface contaminant transport model. The Extended Kalman filter works in a two-step process, the first step is the prediction update and the second step provides the measurement update. Since the Extended Kalman filter is recursive in nature, it can function in real time using only the present input measurements and the previously calculated state.

In this study, the Extended Kalman filter which is stochastic in nature combines both the observation information and the system model. Based on twelve observation data points in the

model domain the results for the stochastic models were generated. The observation data serves as a guide to the system model to give accurate estimates that are much closer or more nearer to the true value. At each time step the twelve observations points were sampled to estimate the optimal contaminant concentration.

Figure 4.4, Figure 4.5 and Figure 4.6 show the contours of the contaminant plume predictions of the Extended Kalman filter at time step 10, 30 and 50, respectively. It can be seen that the prediction results of the Extended Kalman filter are closer to the true value than that of the deterministic model.

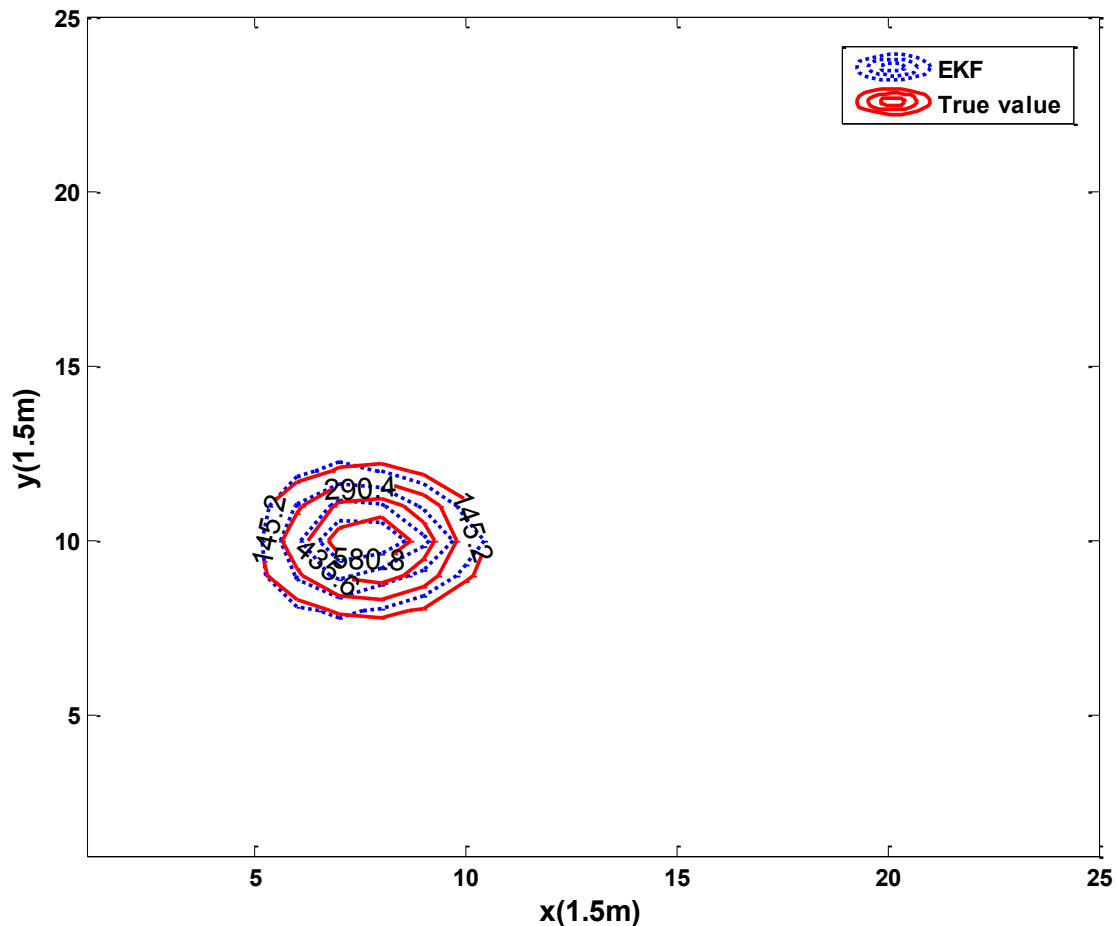


Figure 4.4. Comparison of EKF results and true value at time step 10.

The accuracy of the Extended Kalman filter relative to the deterministic model can be associated to the fact that it uses the observation data which adjusts the system model to project the optimal state while the deterministic model solely relies on its systems of equations, boundary and initial conditions to predict the state. The variability in the hydraulic parameters are accounted for by the stochastic nature of the Extended Kalman filter, which enables it to predict irregular contour shapes which conforms to the true value. The Extended Kalman filter is more randomized in nature than the deterministic model results which have comparatively smooth contours.

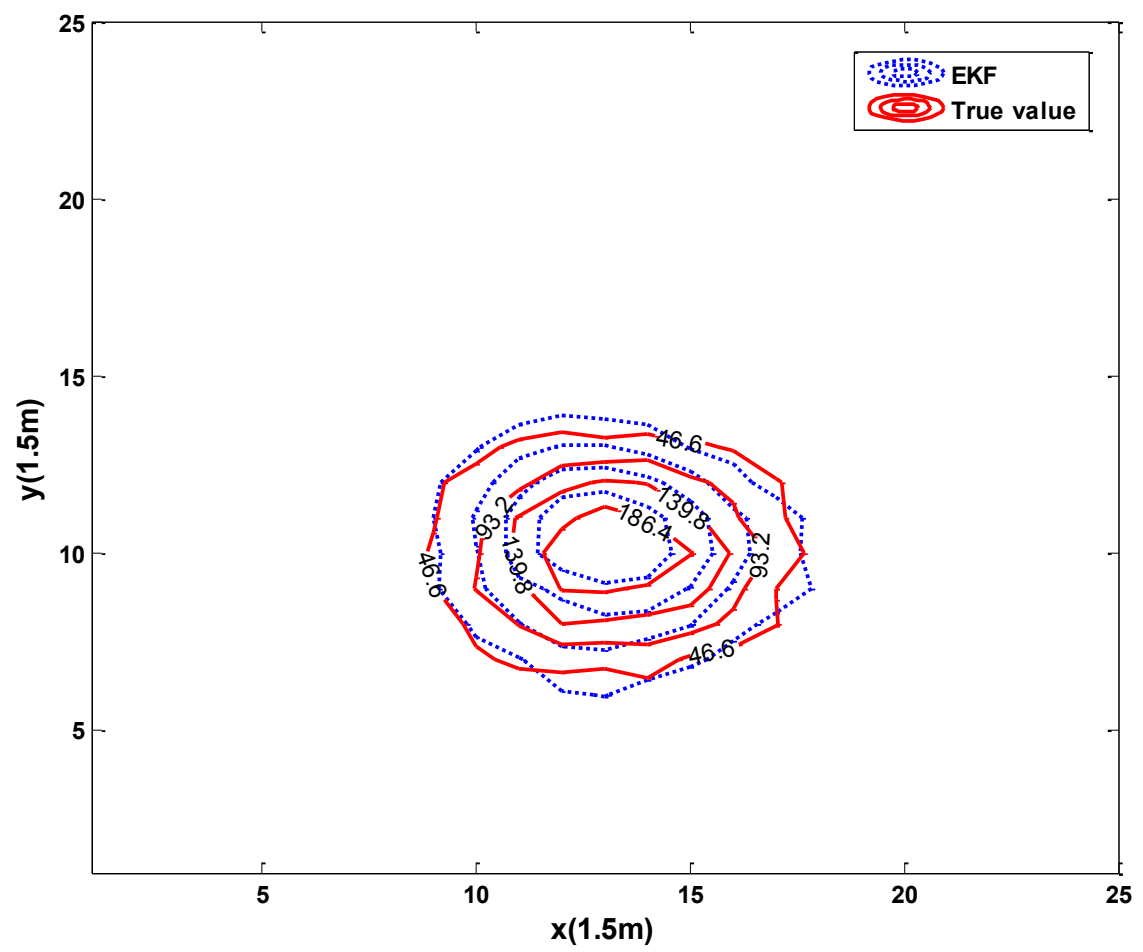


Figure 4.5. Comparison of EKF results and true value at time step 30.

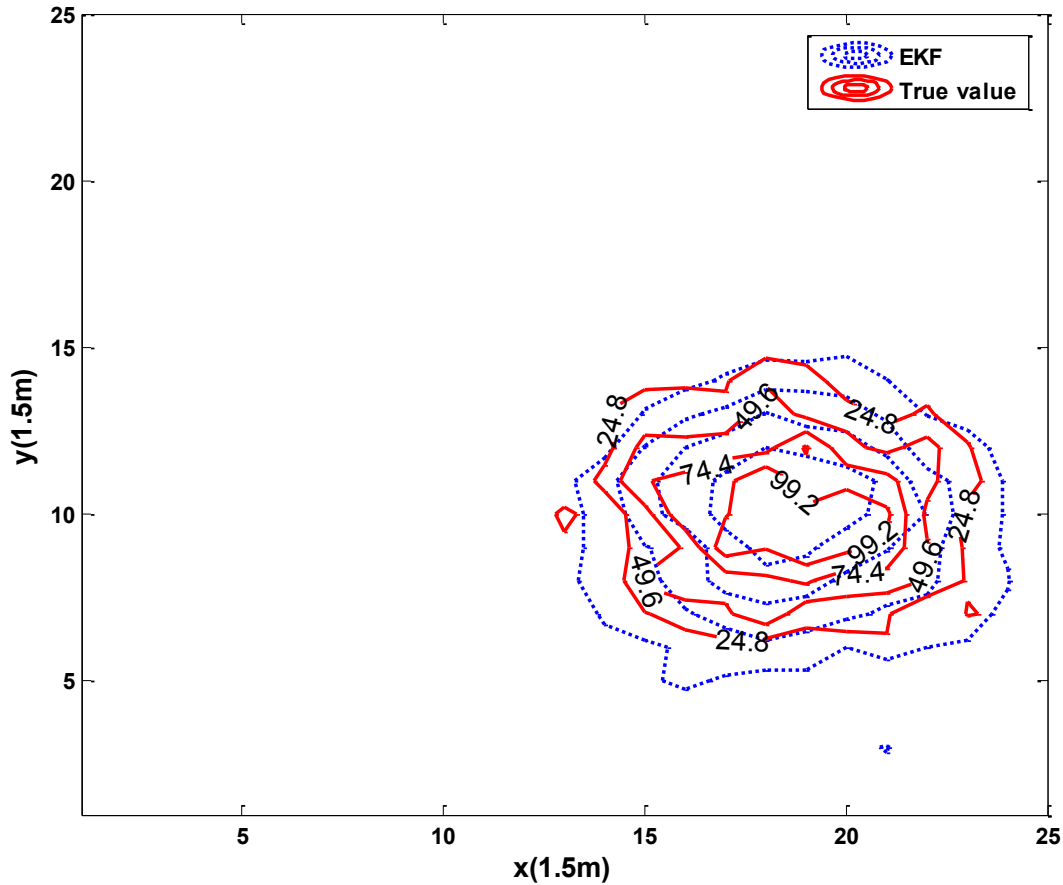


Figure 4.6. Comparison of EKF results and true value at time step 50.

4.4 Simulation Output of Adaptive Extended Kalman Filter

Figure 4.7, Figure 4.8 and Figure 4.9, which represent the contours of the contaminant plume profile from the Adaptive Extended Kalman filter for time steps 10, 30 and 50, respectively, had much better prediction accuracy than the deterministic model and the Extended Kalman filter model. The Adaptive Extended Kalman filter data assimilation scheme like the Extended Kalman filter also uses observation information to predict the state. The introduction of the adaptive filtering scheme into the Extended Kalman filter was successful by giving better prediction than the non-Adaptive Extended Kalman filter.

An effective adaptive system is created by the implementation of the Innovation Covariance Scaling and Gain Correction (ICS-GC). The error covariance and the optimal Kalman gain are adjusted by a scale factor greater than one (Fathabadi et al., 2009). The Adaptive Extended Kalman filter produces faster and smoother convergence than the Extended Kalman filter (Myers et al., 2012). The Adaptive Extended Kalman filter works better than the deterministic model and the Extended Kalman filter in terms of prediction accuracy.

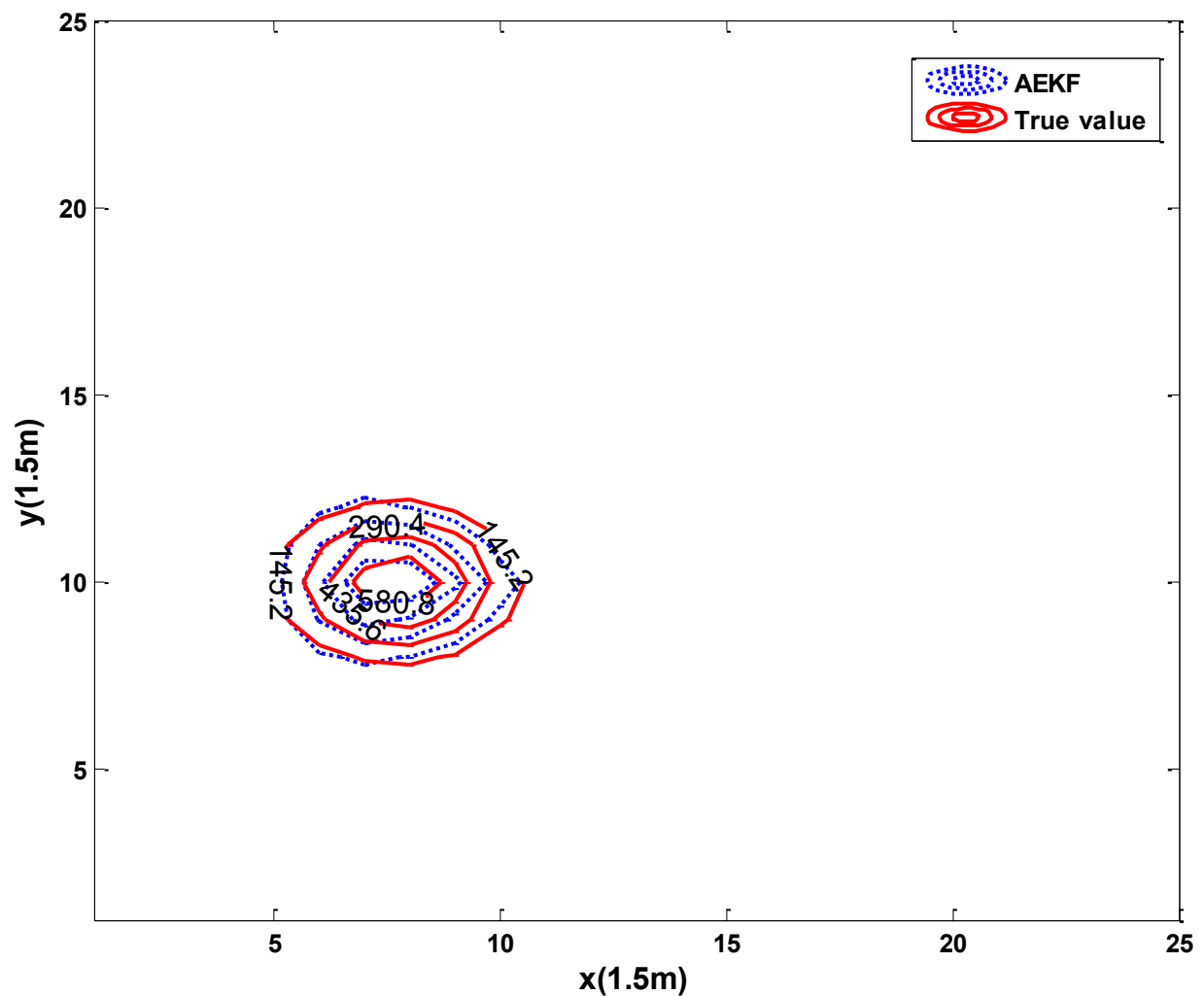


Figure 4.7. Comparison of AEKF results and true value at time step 10.

The Adaptive Extended Kalman filter as a data assimilation scheme combines observation data and model dynamics to give an improved prediction of the state at discrete time and spatial points. The Adaptive Extended Kalman filter reduces the effect of inaccuracies in the initial process noise covariance by assigning less weight to the system model (Hu et al. 2003).

From Figure 4.7, Figures 4.8 and Figures 4.9, it can be realized that the adaptive and forgetting factors used in the Innovation Covariance Scaling and Gain Correction (ICS-GC) adaptive scheme by tuning the system error covariance and the optimal Kalman gain improves the accuracy of the filter prediction.

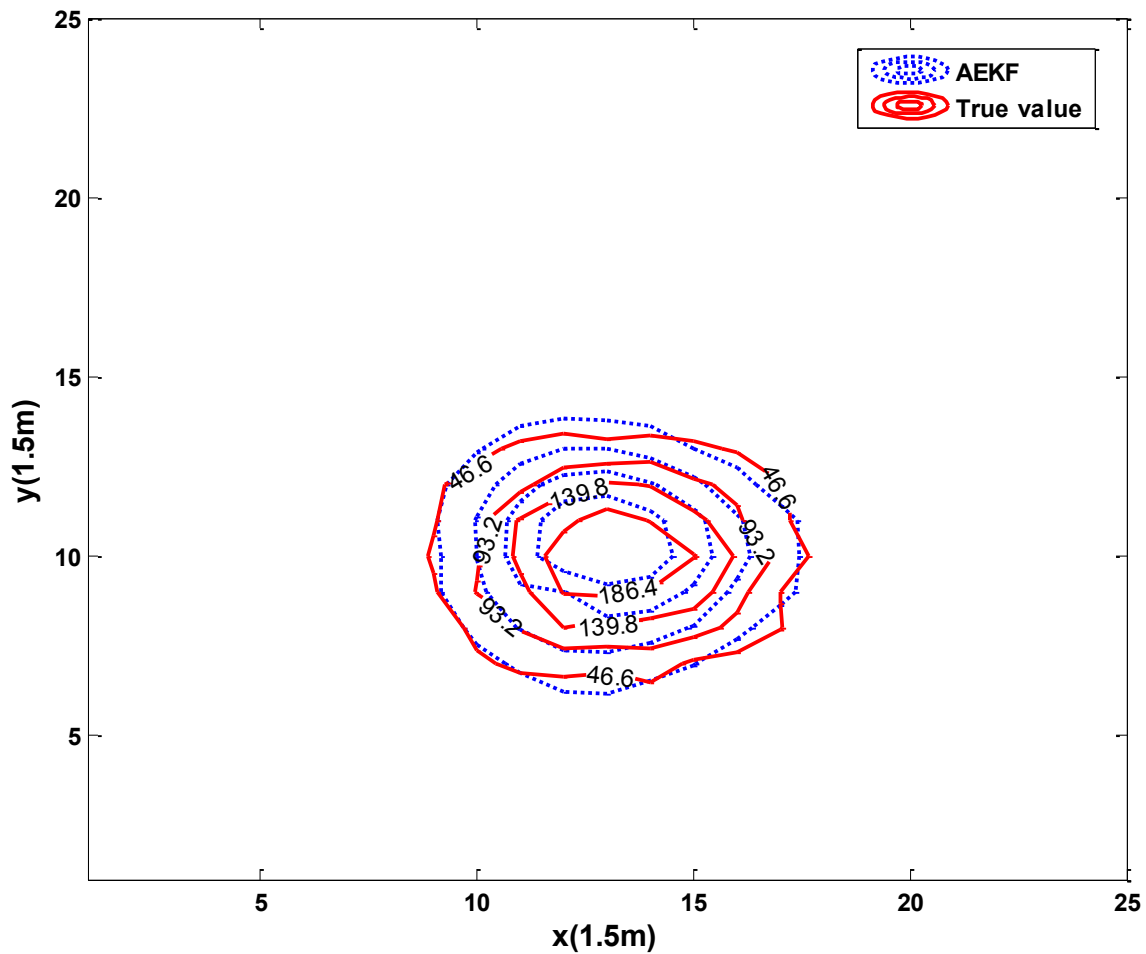


Figure 4.8. Comparison of AEKF results and true value at time step 30.

The prediction results of the Adaptive Extended Kalman filter are also closer to the true value than both the Extended Kalman filter and the deterministic model. The Adaptive Extended Kalman filter is irregular in nature as exhibited by the Extended Kalman filter which makes the prediction quite similar to true field data. At time step 10 the prediction results seem to give the relatively least error and the slight deviation witnessed at time step 50 can be due to the smaller concentrations present at that time.

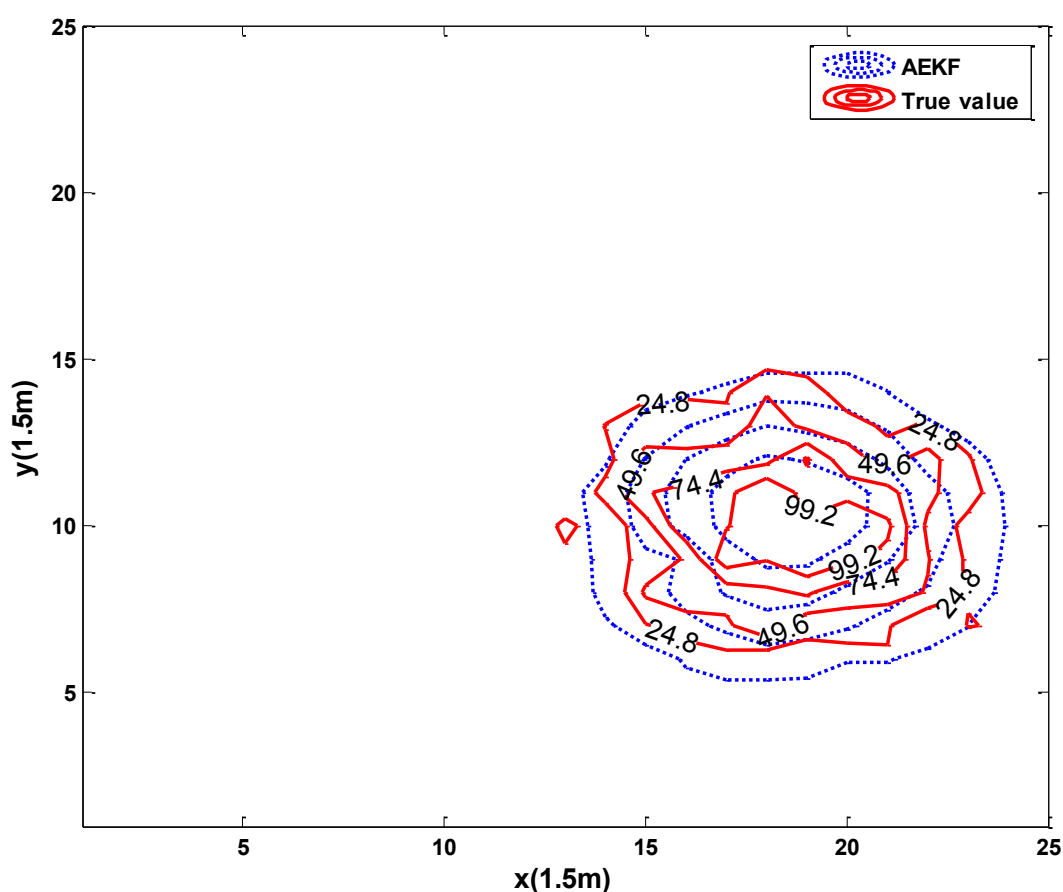


Figure 4.9. Comparison of AEKF results and true value at time step 50.

At time steps 10, 30 and 50 the highest contaminant concentration were found to be 580.8 mg/L, 186.4 mg/L and 99.2 mg/L, respectively. It can be said that both the Adaptive Extended Kalman filter and the Extended Kalman filter, which are stochastic in nature and use observation

information give a better prediction than the deterministic model which is solely based on its system of equations. The closeness of the Adaptive Extended Kalman filter to the true value is an indication of improvement in the system model by the introduction of the adaptive technique thereby providing a more accurate prediction.

Figure 4.10, Figure 4.11 and Figure 4.12 show the concentration profiles by the various models in three dimensional at time step 10, 30 and 50, respectively to give a clearer representation of the concentration profiles. The true value was assigned a velocity higher than the velocity used in the deterministic model which makes the true value to move a little faster than the deterministic model.

At time step 10, the peak contaminant concentration estimated by the true value was around 580.8 mg/L and the peak concentration predicted by the Adaptive Extended Kalman filter, the Extended Kalman filter and the deterministic model were 600 mg/L, 599.5 mg/L and 790 mg/L, respectively. The deterministic model, the Adaptive Extended Kalman filter and the Extended Kalman filter gave a prediction error of about 26%, 3.2% and 3.1%, respectively, relative to the true solution. From the above discussion, it can be realized that the deterministic model gave the highest prediction error, followed by the Adaptive Extended Kalman filter and then the Extended Kalman filter. The slight superiority of the Extended Kalman filter over the Adaptive Extended Kalman filter can be attributed to the inaccurate estimate of the process and observation noise covariances by manipulating the system error covariance, P_t and the optimal Kalman gain, K_t by the use of adaptive and forgetting factors in the adaptive scheme.

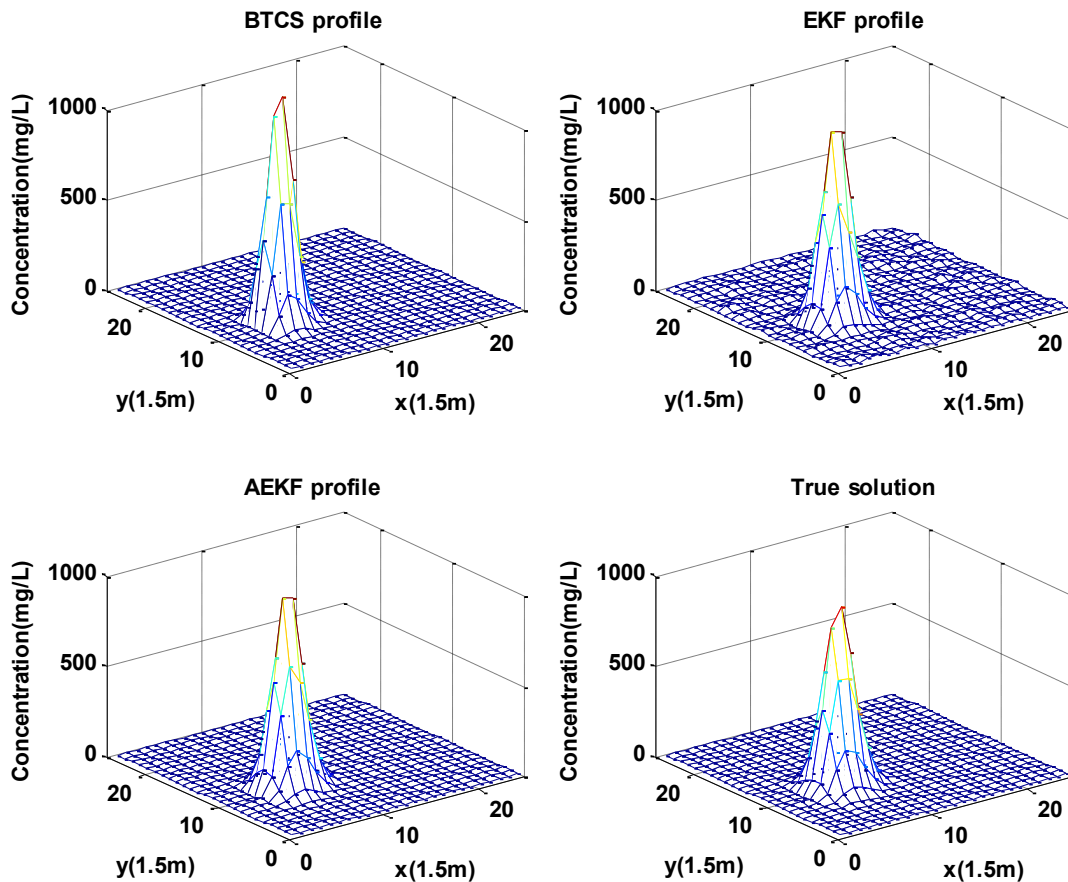


Figure 4.10. Comparison of contaminant concentration prediction of BTCS, EKF, AEKF and True value at time step 10.

At time step 30, the peak concentration predicted by the true value was approximately 186.4 mg/L which was closely predicted by the Adaptive Extended Kalman filter and the Extended Kalman filter to be 190 mg/L and 200 mg/L, respectively while that predicted by the deterministic model was approximately 350 mg/L. Relative to the true value, the Adaptive Extended Kalman filter, Extended Kalman filter and the deterministic model gave a prediction error of approximately 1.9%, 6.8% and 46.7%, respectively. Relative to the deterministic model, the Extended Kalman filter reduces the error in prediction by 39.9% while the Adaptive Extended Kalman filter reduces the error in prediction by 44.8%, indicating that the Adaptive scheme has slightly improved the performance of the Extended Kalman filter by 4.9%.

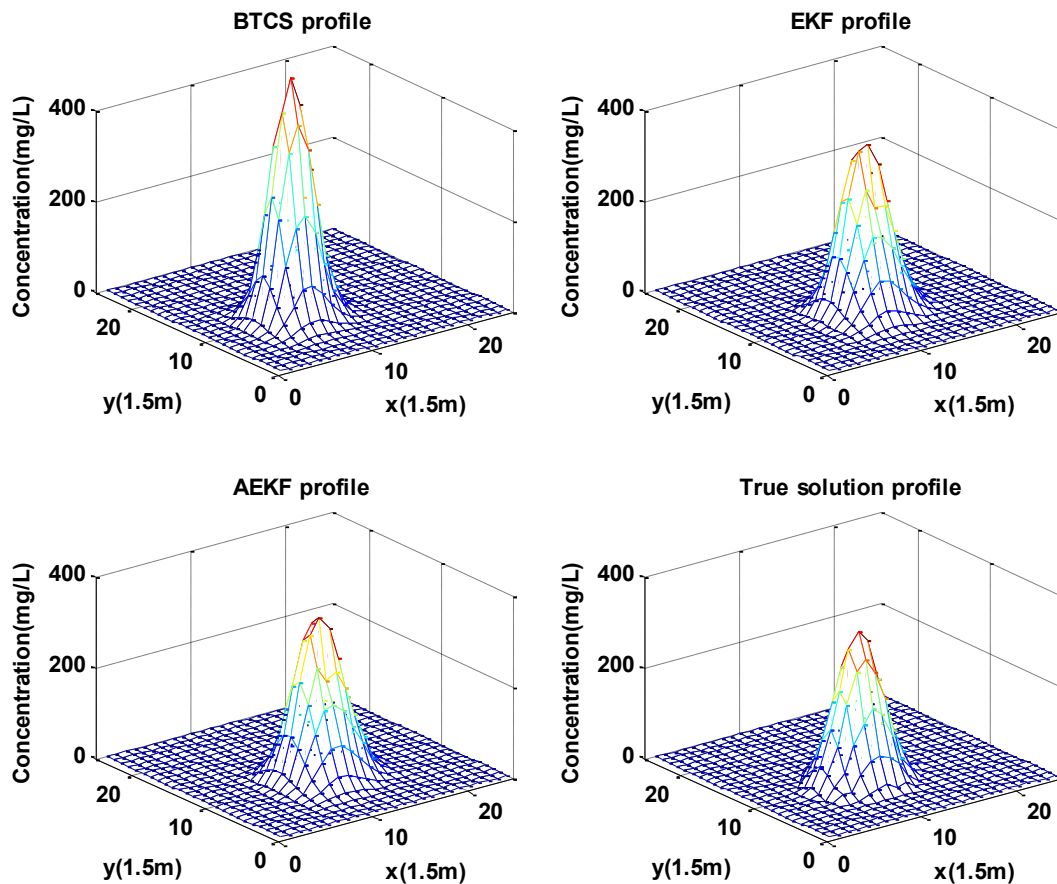


Figure 4.11. Comparison of contaminant concentration prediction of BTCS, EKF, AEKF and True value at time step 30.

Figure 4.12 shows the mesh profile at time step 50, indicating the peak concentration of the true value, the Adaptive Extended Kalman filter, the Extended Kalman filter and the deterministic model. At this stage it can be realized that, there is a continuous reduction in the contaminant concentration as it migrates from one time step to another time step. At the end of the simulation the true value peak concentration was approximately 99.2 mg/L, which was closely predicted by the Adaptive Extended Kalman filter and the Extended Kalman filter to be 110 mg/L and 150 mg/L respectively, whereas the deterministic model predicted relatively higher peak concentration of 240 mg/L. As discussed earlier on, the Adaptive Extended Kalman

filter is closer to the true value than both the Extended Kalman filter and the deterministic model indicating that the initialization of the adaptive filtering scheme was successful in bringing down the prediction error of the Extended Kalman filter scheme.

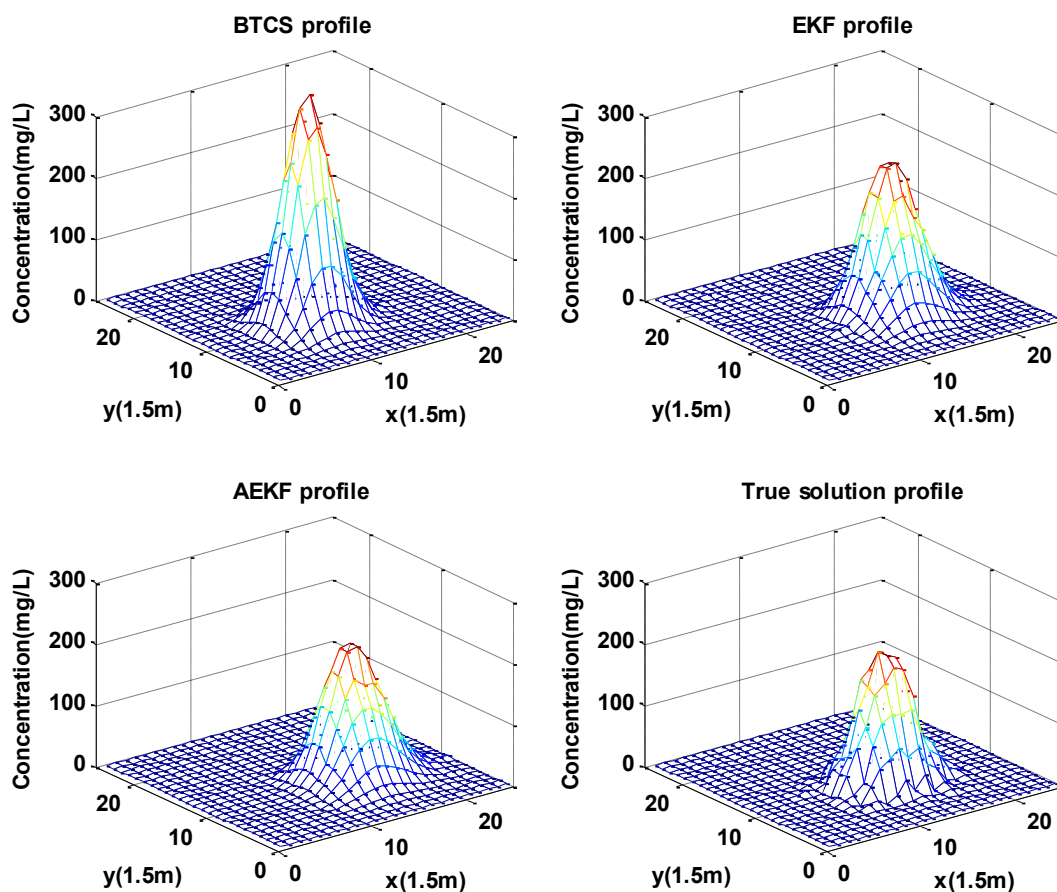


Figure 4.12. Comparison of contaminant concentration prediction of BTCS, EKF, AEKF and True value at time step 50.

The higher peak concentration of the deterministic model can be due to the inaccurate hydrologic parameter used in the model. The true value was also assigned a velocity which was 20% higher than the velocity used in the deterministic model. Despite the fact that hydraulic parameters and initial conditions may be erroneous, both filters can utilize observation information to project the optimal contaminant concentration with minimum deviation.

As shown in Figure 4.10, Figure 4.11 and Figure 4.12, the trend indicates a reduction in peak concentration as the contaminant migrates from one time step to the other. The reduction of the contaminant concentration can be attributed to processes such as dispersion, time rate release of contaminant, chemical processes, advection of contaminant, sorption, dilution, diffusion and other factors that affect the extent and rate of contaminant movement (U.S. Environmental Protection Agency, 1985).

4.5 Analysis of the Prediction Models Effectiveness

The effectiveness and accuracy of the deterministic, Extended Kalman filter and Adaptive Extended Kalman filter schemes were conducted using root mean square error. Figure 4.13 shows the RMSE profile of all the approaches used in this study. An average prediction error of approximately 29.9 mg/L, 21.3 mg/L and 18.2 mg/L were obtained for the deterministic model, the Extended Kalman filter the Extended Kalman filter and the Adaptive Extended Kalman filter, respectively for the entire simulation period when compared with the true solution. However, at the end of the simulation, the prediction error for the deterministic model was 28 mg/L while the Extended Kalman filter and the Adaptive Extended Kalman filter were reduced to 18 mg/L and 11 mg/L in the order given. The Extended Kalman filter improved the prediction by an average of 28.8 % relative to deterministic model while the Adaptive Extended Kalman filter improved the prediction by an average of 39.1% relative to deterministic model for the entire simulation period.

Relative to the numerical results, it can be realized that the Adaptive Extended Kalman filter reduces the errors in prediction by 10.3% on the average compared to the Extended Kalman filter for the entire simulation period. It is evident in Figure 4.13 that the filters gave more accurate estimation in a successful manner by assimilating observation information into the

system. Between time-steps ten and twenty, the Extended Kalman filter appears to perform better than the Adaptive Extended Kalman filter, but after time step twenty the Adaptive Extended Kalman filter gave the least prediction error. It can also be said that at the end of the simulation, the introduction of the Extended Kalman filter improved the deterministic model prediction by reducing the model error from 28 mg/L to 18 mg/L, thus improving the prediction accuracy by about 35%.

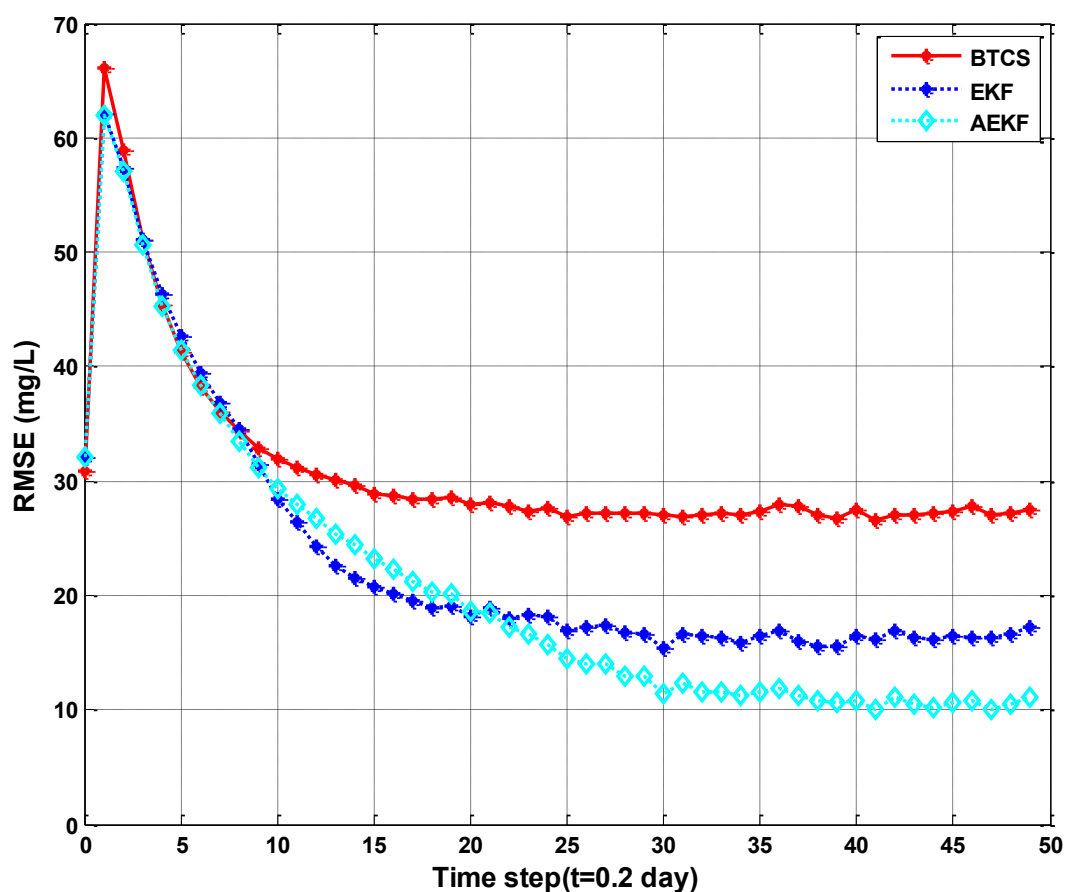


Figure 4.13. Root Mean Square Error (RMSE) profile for BTCS, EKF and AEKF.

A further comparison in Figure 4.13 shows that the Adaptive Extended Kalman filter scheme further brought down the prediction error of the Extended Kalman filter scheme from 18 mg/L to 11 mg/L at the end of the simulation period hence ameliorating prediction accuracy by

approximately 38.9%. From the above discussion, it can be realized that the Adaptive Extended Kalman filter is superior in predicting contaminant transport in the subsurface than the Extended Kalman filter and the deterministic model.

4.6 Stability and Convergence Analysis of the Prediction Models

Figure 4.14, Figure 4.15 and Figure 4.16 represent the stability and convergence of the deterministic model, the Extended Kalman filter and the Adaptive Extended Kalman filter for a series of repeated runs.

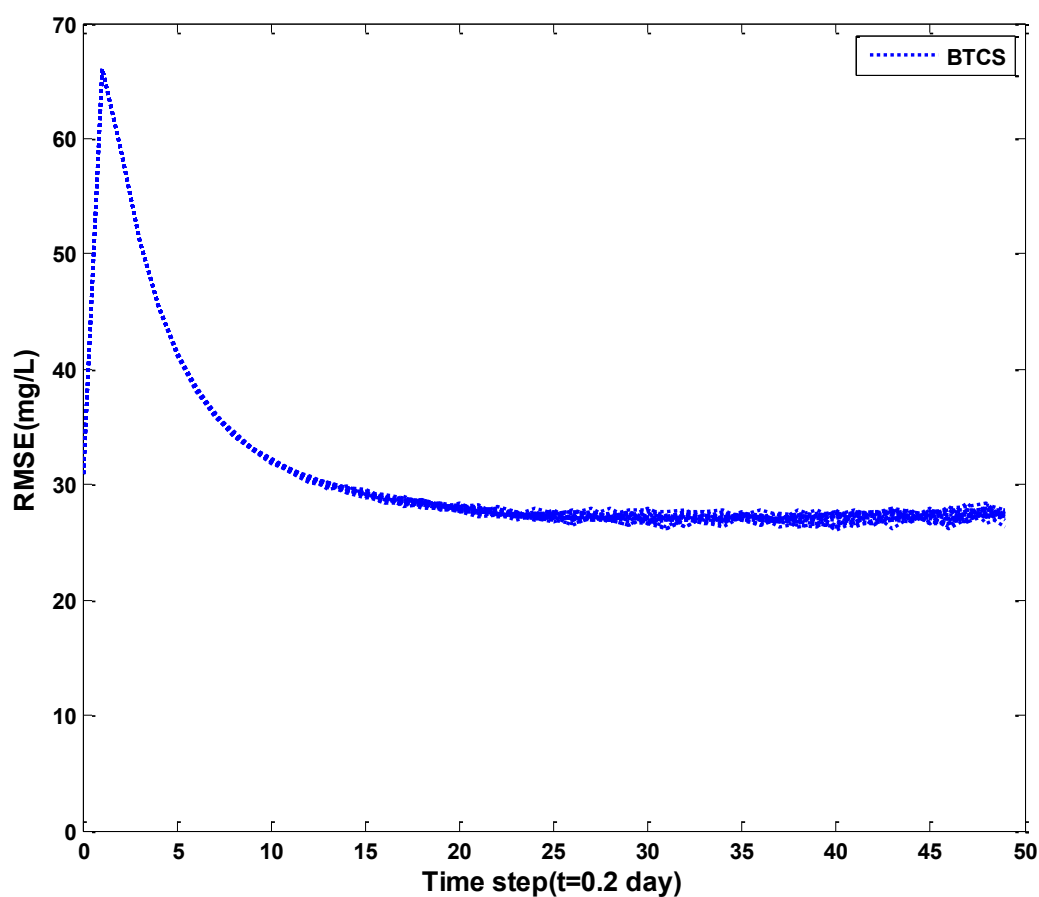


Figure 4.14. Fifteen runs of RMSE profile for BTCS

The Adaptive Extended Kalman filter has been used to increase the stability and the convergence performance of the filter in order to avoid divergence of the filter by reducing the errors that emanate from the process and observation noise covariance.

In this study, the stability and Convergence of the deterministic model, Extended Kalman filter and the Adaptive Extended Kalman filter are analyzed by performing multiple runs of the root mean squared-error profile. From Figure 4.15 and Figure 4.16, the Adaptive Extended Kalman filter and Extended Kalman filter became stable and converge after time step 20 during the simulation period.

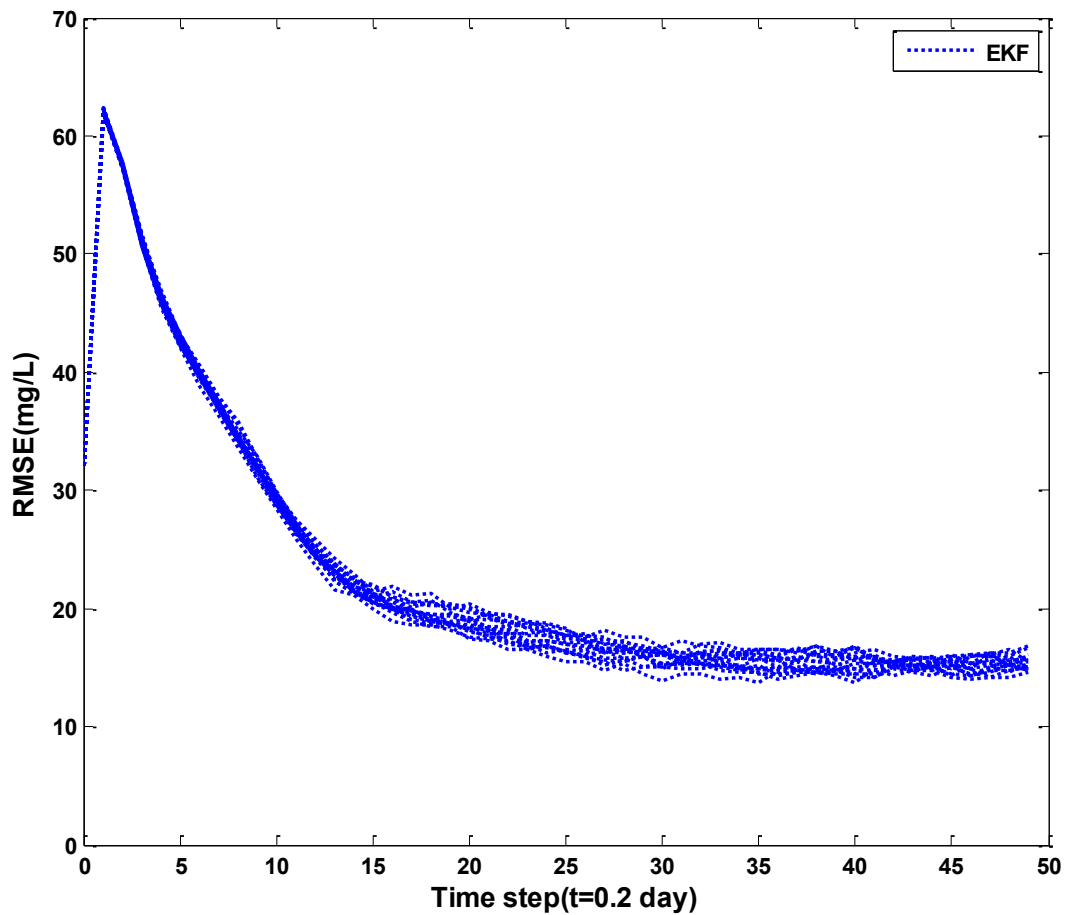


Figure 4.15. Fifteen runs of RMSE profile for EKF.

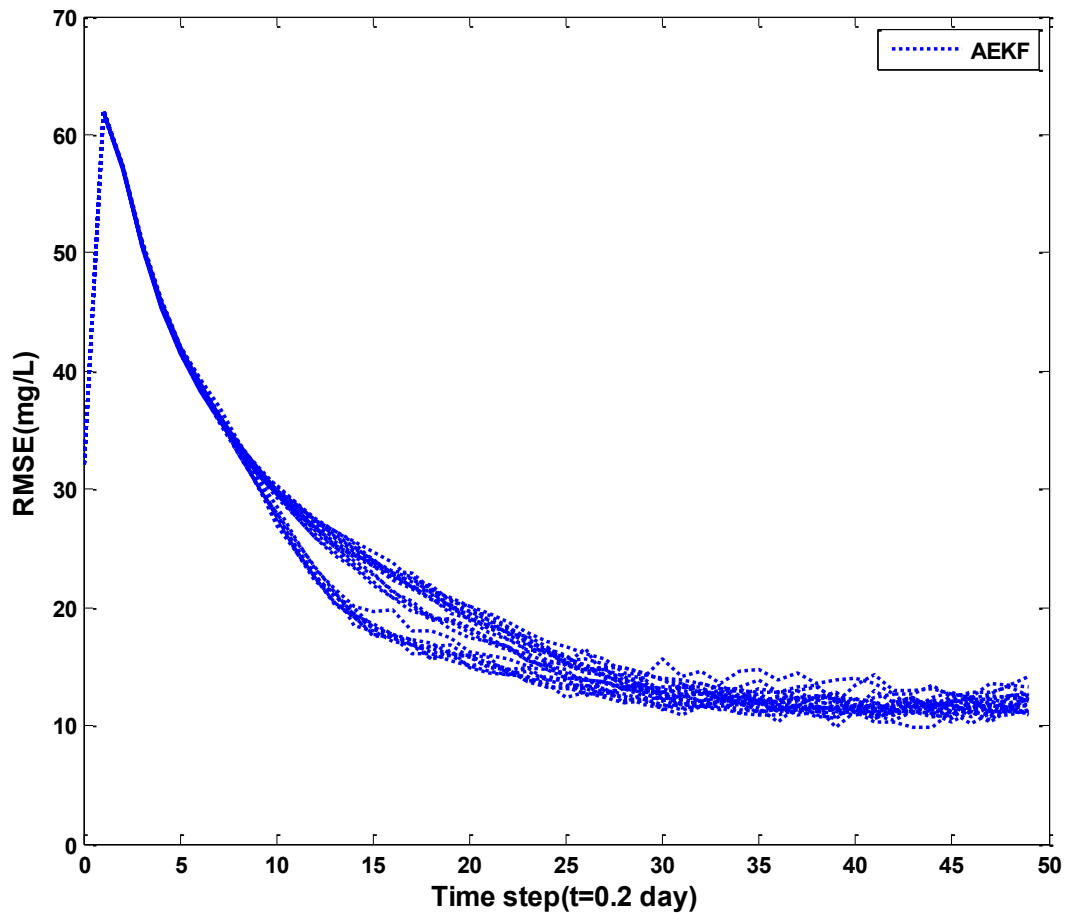


Figure 4.16. Fifteen runs of RMSE profile for AEKF.

4.7 Process Noise Adjustment

In this study, the process noise standard deviation (PNSD) was set to 5% to portray the stochastic characteristic of the true field. Sensitivity tests were further carried on to examine the influence of the process noise standard deviation (PNSD) on the prediction of the Adaptive Extended Kalman filter by simulating the filter with different process noise standard deviations. The sensitivity test was conducted by changing the process noise standard deviation to 1%, 7%, 14% and eventually to 21% while maintaining the same observation noise standard deviation.

Figure 4.16 indicates the performance of the root mean square error profile of the Adaptive Extended Kalman filter when the sensitivity test was performed on the process noise

standard deviation by setting it to 1%, 7%, 14% and 21%, respectively for a constant observation noise standard deviation (ONSD) of 2.5%. From the RMSE profile it can be said that after time step 5 the difference in the results started to manifest and carried on until the last time step.

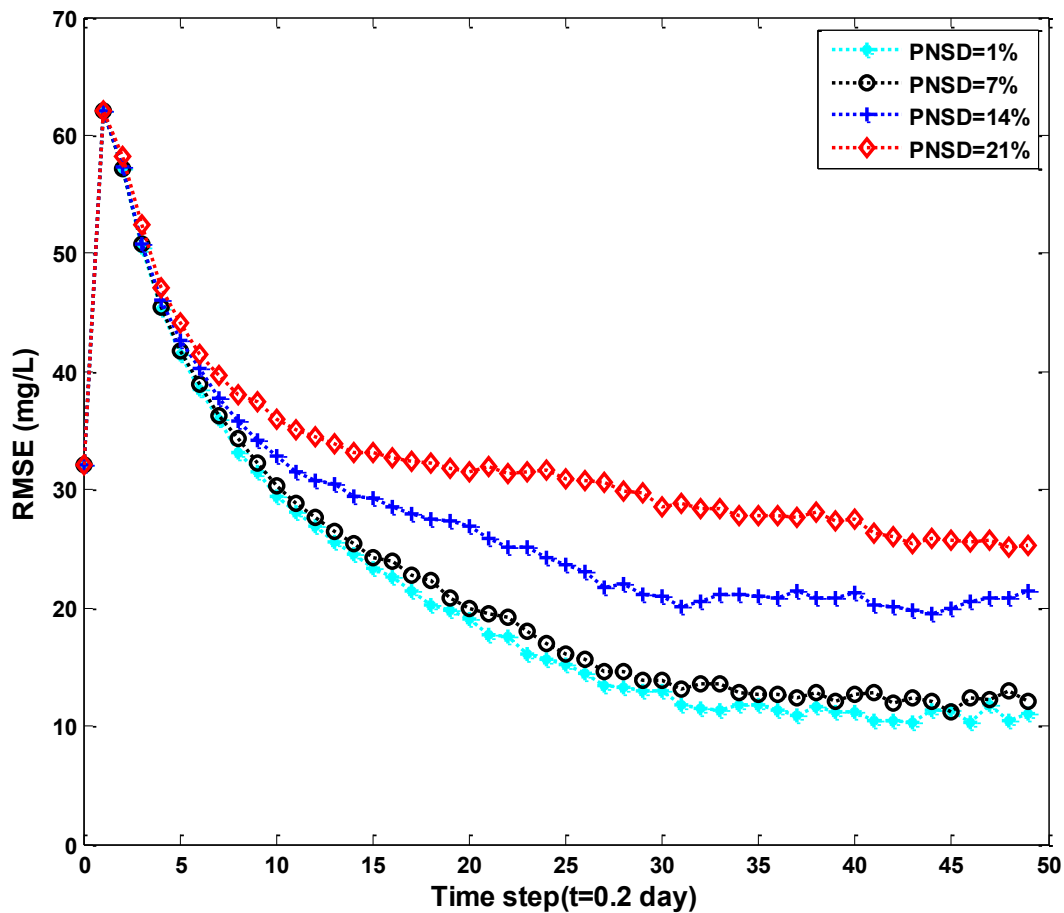


Figure 4.17. RMSE profile of AEKF for different process noise standard deviation (PNSD) values.

At the end of the simulation, using a process noise standard deviation of 1% improved the performance of the filter by approximately 15.4%, 47.6% and 56% relative to the RMSE results obtained with a process noise standard deviation of 7%, 14% and 21% respectively. From the

results, it can be said that the smaller the process error introduced into the filtering, the smaller the error that will be associated with the estimation results and vice versa.

4.8 Observation Noise Adjustment

Sensitivity analysis was again conducted on the observation noise standard deviation (ONSD) to examine the impact it has on the model results. Similitude to the process noise, the observation noise standard deviation for the Adaptive Extended Kalman filter was varied while the process noise standard deviation was treated as a constant. The standard deviation of observation noise (ONSD) was set at 1%, 7 %, 14% and 21%, respectively while maintaining the same process noise standard deviation of 5%.

Figure 4.17 shows the performance of the root mean square error profile of the Adaptive Extended Kalman filter when the sensitivity test was performed on the observation noise standard deviation. From the results, it can be observed that the respective Adaptive Extended Kalman error filters were closer after time step 5 until time step 30 where there was a significant difference in performance of the result of the filter until the end of the simulation. The observation noise standard deviation of 7% had a better output than the observation noise standard deviation of 1% from time step 8 to time step 32, even though from time step 35 to the end of the simulation the RMSE profile of the 1% observation noise standard deviation comes out to be slightly better than the 7% observation noise standard deviation.

From the RMSE profile results between the observation noise standard deviation of 14% and 21%, it can be said that from time step 15 to time step 25, the observation noise standard deviation of 21% appears to perform slightly better than the observation noise standard deviation of 14%. But from time step 25 to the end of the simulation the observation noise standard deviation of 14% had an improved output than the observation noise standard deviation of 21%.

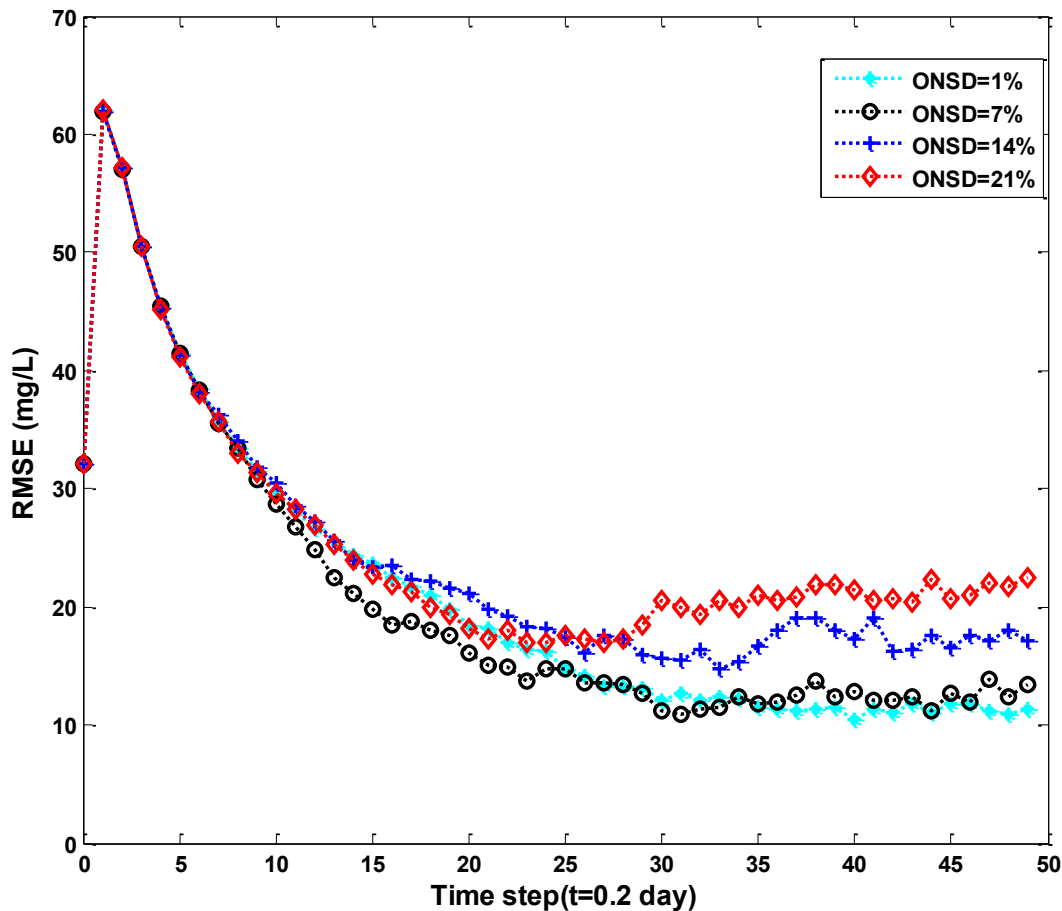


Figure 4.18. RMSE profile of AEKF for different observation noise standard deviation (ONSD) values

Also, comparing the RMSE profile results of the observation noise standard deviation of 7% and that of 14% it be observed that the observation noise standard deviation of 7% is superior in performance over the observation noise standard deviation of 14%. At the end of the simulation, the RMSE result using an observation noise standard deviation of 1% relative to the standard deviation of 7%, 14% and 21% ameliorate the performance of the filter by approximately 21.4%, 38.9% and 52.2%, respectively.

Arrangement of all the four scenarios in order of superiority in performance will be the observation noise standard deviation with the 1%, followed by 7%, last but not the least 14% and

finally 21% the least of them all. From the above discussion, it can be said that the higher the observation noise standard deviation introduced into the filtering process, the larger the error associated with the estimation results.

The Adaptive Extended Kalman filter was further investigated by looking at the impact the window size has on the innovation covariance; therefore a sensitivity test was conducted by estimating the innovation covariance with different window sizes. Figure 4.19 shows the performance of the Adaptive Extended Kalman filter with different window size.

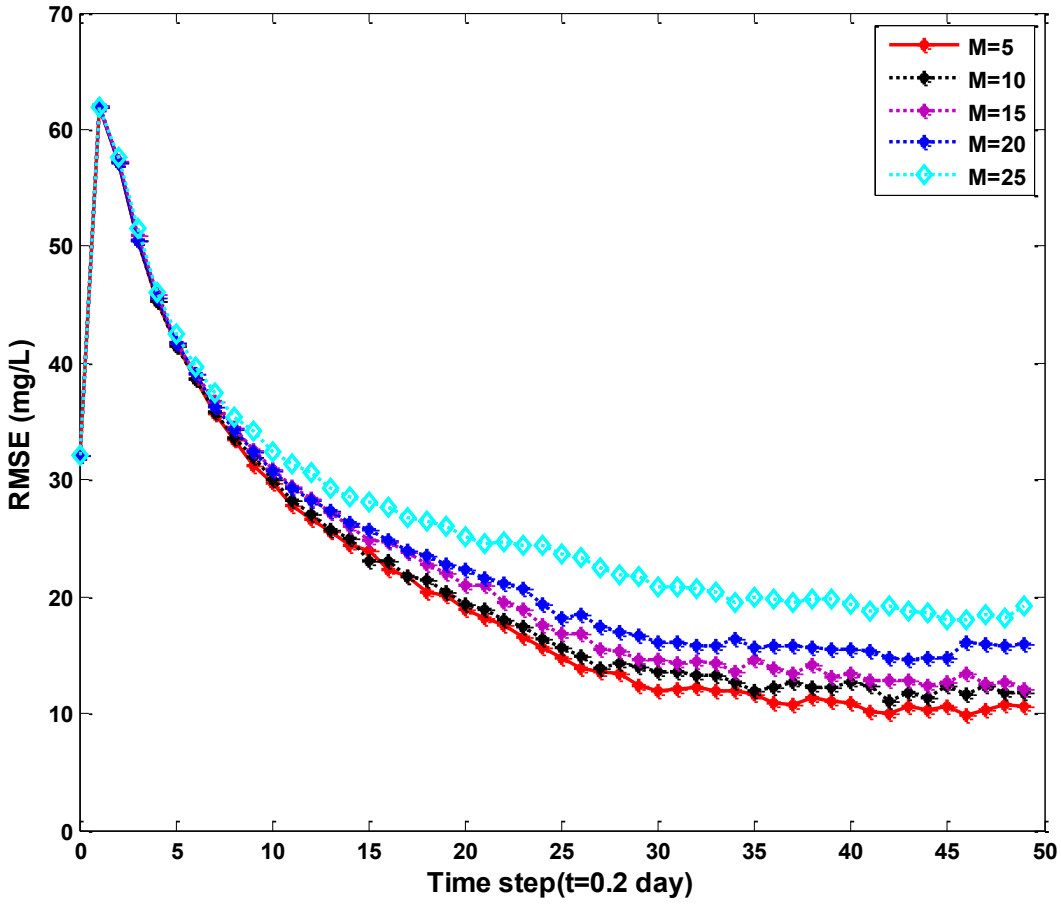


Figure 4.19. Comparison of AEKF performance with different window sizes.

From the RMSE profile shown in Figure 4.19, where the Adaptive Extended Kalman filter was used with window size ranging from 5,10,15,20 and 25, it was observed that the

Adaptive Extended Kalman filter with window size of 25 had the highest prediction error of approximately 19 mg/L while a window size of 5 had the least prediction error of about 11 mg /L. It can also be realized that on the average, a window size of 10 had a slight better output than a window size of 15 even though at the end of the simulation they seem to give a similar prediction error of 12 mg/L. Also, comparing the performance of a window size of 15 and that of 20, it is obvious from the RMSE profile that a window size of 15 performs better than a window size of 20. It can be concluded from this investigation that, the higher the window size, the higher the prediction error which indicates that a window size of 5 gave the optimal prediction. It must also be noted that using a very small window size will make the Adaptive Extended Kalman filter less effective, since the true innovation covariance may not be accurately estimated.

CHAPTER 5

Conclusion and Future Research

Human activity that releases chemicals or waste to the environment either intentionally or accidentally has the potential to pollute groundwater. Groundwater contamination has been major concerns in recent times since majority of the people in the world depend on groundwater as a source of drinking water. Modeling the behavior of contaminants in groundwater is essential in predicting the fate of the pollutants in order for management to take critical decision in the mitigation process and in risk assessment.

In this study, a two-dimensional subsurface advection-dispersion model for the transport of contaminant was used to examine the accuracy and effectiveness of the numerical, the Extended Kalman filter and the Adaptive Extended Kalman filter results relative to the true value results. MatLab code was formulated based on the partial differential equation (advection-dispersion equation for a two dimensional transport).

Contour profiles of the deterministic model, the Extended Kalman filter and the Adaptive Extended Kalman filter in comparison with the true value at various time steps were plotted. The prediction by the deterministic model distinctly moves slower than the true value. The results of numerical models are normally idealistic to apply practically as a result of its lack of ability to simulate true field conditions. The contaminant plume of the deterministic model has comparatively smooth shape as a result of the approximation made to it and this approximation introduce errors into the deterministic model thereby affecting the accuracy and precision of the prediction.

Despite the fact that numerical model is useful in predicting the fate and transport of contaminants in groundwater, the complex nature of the subsurface environment makes it

extremely difficult to give accurate prediction. The deterministic model assumes constant parameters and homogeneity in generating results, while both the Extended Kalman filter and the Adaptive Extended Kalman filter takes into consideration updating and prediction in results generation.

The Extended Kalman filter and the Adaptive Extended Kalman filter which are stochastic in nature combine both observation information and the system model. It can be seen that the prediction results of the Extended Kalman filter are closer to the true value than that of the deterministic model. Both Adaptive Extended Kalman Filter and Extended Kalman filter are randomized in nature which makes their prediction quite similar to the true field data. The adaptive and forgetting factors used in the Innovation Covariance Scaling and Gain Correction adaptive scheme by tuning the system error covariance and the optimal Kalman gain improves the accuracy of the filter prediction.

The effectiveness and accuracy of the deterministic, Extended Kalman filter and Adaptive Extended Kalman filter schemes were conducted using root mean square error. The Extended Kalman Filter improved the prediction by an average of 28.8 % relative to deterministic model while the Adaptive Extended Kalman filter improved the prediction by an average of 39.1% relative to deterministic model for the entire simulation period in the 37.5 by 37.5 space domain using twelve observation points.

At the end of the simulation, the introduction of the Extended Kalman filter improved the deterministic model prediction by reducing the model error from 28 mg/L to 18 mg/L, thus improving the prediction accuracy by about 35.7 %. Although the Extended Kalman filter was successful in reducing the errors in the deterministic model, the Adaptive Extended Kalman filter scheme further reduced the prediction error of the Extended Kalman filter from 18 mg/L to

11mg/L hence ameliorating prediction accuracy by approximately 38.9%. Overall, the implementation of the Adaptive Extended Kalman filter was successful in improving the prediction accuracy of the deterministic model by about 60.7% which shows a substantial improvement in the prediction of the contaminant concentration. The study revealed that the Adaptive Extended Kalman filter performs better than the Extended Kalman filter.

Sensitivity tests were further carried on to examine the influence of the process noise standard deviation (PNSD) on the prediction of the Adaptive Extended Kalman filter by simulating the filter with different process noise standard deviations. The investigation revealed that the performance of the Adaptive Extended Kalman filter works better when the process noise standard deviation is made minimum by using 1% compared to when it is adjusted to 7%, 14% and 21%.

Also, sensitivity analysis was again conducted on the observation noise standard deviation (ONSD) to examine the impact it has on the model results. The RMSE result using an observation noise standard deviation of 1% relative to the standard deviation of 7%, 14% and 21% ameliorate the performance of the filter by approximately 21.4%, 38.9% and 52.2%, respectively. The investigation shows that the higher the process and observation noise standard deviation introduced into the filtering process, the larger the error associated with the estimation results, hence choosing the appropriate process and observation noise standard deviation can have a significant impact on filter performance.

The stability and convergence of the models were analyzed by performing multiple runs of the root mean squared-error profile. The investigation conducted on the window size shows that, as the window size increases, the higher the prediction error associated with the Adaptive Extended Kalman filter. Future work will focus on the use of Adaptive Extended Kalman filter

with time correlated errors under three-dimensional subsurface environment and also the adaptive techniques will be introduced into the Ensemble Kalman filter.

References

- Bear, J. (1972). *Dynamics of fluids in porous media*. Elsevier, New York, USA.
- Becerra, V. M., Roberts, P. D., and Griffiths, G. W. (2001). "Applying the extended kalman filter to systems described by nonlinear differential-algebraic equations." *Control Engineering Practice*, 9, 267-281.
- Branicki, M., Gershgorin, B., and Majda, A. J. (2012). "Filtering skill for turbulent signals for a suite of nonlinear and linear extended kalman filters." *Journal of Computational Physics*, 231, 1462–1498.
- Breger, D. S., Hubbell J. E., and Hasnaoui, H. E. and Sunderland, J. E. (1996). "Thermal energy storage in the ground, comparative analysis of heat transfer modeling using u-tubes and boreholes." *Solar Energy*, 56(6), 493-503.
- Bryant, S., Schechter, R., and Lake, L. (1987). "Mineral sequences in precipitation/dissolution waves." *AIChE J.*, 33, 1271-1287.
- Budhiraja, A., Chen, L., and Lee, C. (2007). "A survey of numerical methods for nonlinear filtering problems." *Physica D*, 230, 27–36.
- Chang, S. Y., and Jin A. (2005). "Kalman filtering with regional noise to improve accuracy of contaminant transport models." *Journal of Environmental Engineering*, 131(6), 971-982.
- Chang, S.Y., and Li, X.P. (2006). "Modeling chlorobenzene leaching from a landfill into a Soil environment using particle filter approach." *Journal of Environmental Informatics*, 12(2),88-95.
- Chang, S. Y., and Latif, S. M. I. (2010). "Extended kalman filtering to improve the accuracy of a subsurface contaminant transport model." *Journal of Environmental Engineering*, 136(5), 466-474.

- Chen, J., and Rutan, S. C. (1996). "Identification and quantification of overlapped peaks in liquid chromatography with UV diode array detection using an adaptive Kalman filter." *Analytica Chimica Acta*, 335, 1-10.
- Cheng, H. P., and Yeh G. T. (1998). "Development and demonstrative application of a 3-D numerical model of subsurface flow, heat transfer, and reactive chemical transport: 3-D hydrogeochem." *Journal of Contaminant Hydrology*, 34, 47-83.
- Domenico, P. A., and Schwartz, F. W. (1998). *Physical and chemical hydrogeology*. Wiley, New York, USA.
- Dria, M., Bryant, S., Schechter, R., and Lake, L. (1987). "Interacting precipitation/dissolution waves, the movement of inorganic contaminants in groundwater." *Water Resources Research*, 23, 2076-2090.
- Eppstein, M. J., and Dougherty, D. E. (1996). "Simultaneous estimation of transmissivity values and zonation." *Water Resources Research*, 32(11), 3321-3336.
- Fathabadi, V., Shahbazian, M., Salahshour, K., and Jargani, L. (2009). "Comparison of adaptive kalman filter methods in state estimation of a nonlinear system using asynchronous measurements." *Proceedings of the World Congress on Eng. and Computer Sc.*, San Francisco, CA.
- Fetter, C.W. (1993). *Contaminant hydrogeology*. Macmillan Publishing Company, New York.
- Fetter, C.W. (1999). *Contaminant hydrogeology*. Prentice-Hall, Upper Saddle River, New Jersey.
- Freeze, R. A., and J. A. Cherry. (1979). *Groundwater*. Prentice-Hall, Englewood Cliffs, New Jersey.

- Geer, F. C. V. (1982). "An equation based theoretical approach to network design for groundwater levels using kalman filters." *International Association of Hydrological Sciences*, 136, 241-250.
- Gelhar, L.W. (1993). *Stochastic subsurface hydrology*. Prentice-Hall, Englewood Cliffs, New Jersey.
- Gerald, E., and Peter, V. (2006). "Frequency-domain adaptive Kalman filter for acoustic echo Control in hands-free telephones." *Signal Processing*, 86, 1140–1156.
- Gerald, W. R. (2011). "Finite difference approximations to the heat equation." Mechanical Engineering Department Portland State University, Portland, Oregon, www.f.kth.se/~jjalap/numme/FDheat.pdf. (assessed: August 15, 2012).
- Girgis, A. A., and Peterson, W. L. (1990). "Adaptive estimation of power system frequency deviation and its rate of change for calculating sudden power system overloads." *IEEE Transactions on Power Delivery*, 5, 585–594.
- Gorelick, S. M., Freeze R.A., Donohue D., and Keely J. F. (1993). *Groundwater contamination optimal capture and containment*. Lewis Publishers, Boca Raton, Florida.
- Guoquan, P. H., and Stergios I. R. (2008). "An observability constrained UKF for improving slam consistency." *Multiple Autonomous Robotic Systems Laboratory, Tech. Rep. 2*, 1-29.
- Hajiyev, C. (2007). "Adaptive filtration algorithm with the filter gain correction applied to integrated INS/radar altimeter." *Proc. of the Institution of Mechanical Engineers, Part G: Journal of Aerospace Engineering*, 221(5), 847-855.
- Han, J., Kim, D., and Sunwoo, M. (2009). "State-of-charge estimation of lead-acid batteries using an adaptive extended kalman filter." *Journal of Power Sources*, 188, 606–612.

- Hesham, M. B., Mohamed, A. E., and Ahmed, E. H. (2009). "Contaminant transport in groundwater in the presence of colloids and bacteria, model development and verification." *Journal of Contaminant Hydrology*, 108, 152–167.
- Hide, C., Michaud, F., and Smith, M. (2004). "Adaptive kalman filtering algorithms for integrating GPS and low cost INS." *IEEE Position Location and Navigation Symposium*, Monterey, CA, 227-233.
- Hu, C., Chen, W., Chen, Y., and Liu, D. (2003). "Adaptive kalman filtering for vehicle navigation." *Journal of Global Positioning System*, 2(1), 42-47.
- Jazwinski, A. H. (1970). *Stochastic processes and filtering theory*. Academic Press, New York.
- Kanivetsky, R. (2000). "Arsenic in minnesota groundwater, hydrogeochemical modeling of the quaternary buried artesian aquifer and cretaceous aquifer systems." 55, Minnesota Geological Survey, Saint Paul.
- Kao, J., Flicker, D., Henninger, R., Ghil, M., and Ide, K. (2003). "Using extended kalman filter for data assimilation and uncertainty quantification in shock-wave dynamics." *IEEE Computer Society Press*, 3-4942.
- Kathleen A. K., and Stephen C. S. (2006). "Analysis and implementation of a neural extended kalman filter for target tracking." *International Journal of Neural Systems*, 16(1), 1-13.
- Khan M. S., and Khaled B. (2009). "Development techniques of multi-agents based autonomous railway vehicle control systems." *Engineering and Technology*, 38, 1515-1524.
- Kim, K.H., and Lee, J.G. (2006). "Adaptive two-stage EKF for INS-GPS loosely coupled system with unknown fault bias." *Journal of Global Positioning Systems*, 5(1-2), 62-69.
- Kinniburgh, D. G., Gale, I. N., Smedley, P. L., Darling, W. G., West, J. M., Kimblin, R. T., Parker, A., Rae, J. E., Aldous, P. J., and O'Shea, M. J. (1994). "The effects of historic

- abstraction of groundwater from the london basin aquifers on groundwater quality.”
Applied Geochemistry, 9(2), 175-196.
- Kolker, A., Haack, S. K., Cannon, W. F., Westjohn, D. B., Kim, M.-J., Nriagu, J., and Woodruff, L.G. (2003). *Arsenic in southeastern Michigan*. Kluwer Academic Publishers, Norwell, Massachusetts.
- Lee, K. S. (2011) “Modeling on the cyclic operation of standing column wells under regional groundwater flow.” *Journal of Hydrodynamics*, 23(3), 295-301.
- Lippiello, V., Siciliano, B., and Villani, L., (2007). “Adaptive extended Kalman filtering for visual motion estimation of 3-D objects.” *Control Engineering Practice*, 15, 123–134.
- Lin, L., Yang, J., Zhang, B., and Zhu, Y. (2010) “A simplified numerical model of 3-D groundwater and solute transport at large scale area.” *Journal of Hydrodynamics*, 22 (3), 319-328.
- Loebis, D., Sutton, R., Chudley, J., and Naeem, W. (2004) “Adaptive tuning of a kalman filter via fuzzy logic for an intelligent AUV navigation system.” *Control Engineering Practice*, 12, 1531–1539.
- Matisoff, G., Khourey, C. J., Hall, J. F., Varnes, A. W., and Strain, W. H. (1982). “The nature and source of arsenic in Northeastern Ohio ground water.” *Ground Water*, 20, 446-456.
- Maybeck, P. S. (1982). *Stochastic models, estimation and control*. Academic Press, New York.
- McLaughlin, D. (2002). “An integrated approach to hydrologic data assimilation: interpolation, smoothing and forecasting.” *Advances in Water Resources*, 25, 1275-1286.
- Meissner, P., Wehrmann, R., and Van der List, J. (1980). “A comparative analysis of Kalman and gradient methods for adaptive echo cancellation.” *AEU, Internat. J. Electronics and Communications*, 34 (12), 485–492.

- Myers, M. R., Jorge, A. B., Yuhas, D. E., and Walker, D. G. (2012). “An adaptive extended kalman filter incorporating state model uncertainty for localizing a high heat flux point source using an ultrasonic sensor array.” *Computer Modeling in Engineering and Sciences*, 83(3), 221-248.
- National Ground Water Association (NGWA) and United States Geological Survey (USGS) (2003). *Ground Water Statistics*. www.ngwa.org. (assessed: July 17, 2012).
- Park, E. E., and Zhan, H. H. (2001). “Analytical solutions of contaminant transport from finite one, two, and three dimensional sources in a finite thickness aquifer.” *Journal of Contaminant Hydrology*, 53(1), 41-61.
- Pye, V. I., and Kelley, J. (1984). *The extent of groundwater contamination in the United States*. National Academy Press, Washington, DC.
- Rogers, B., and Logan, B. E. (2000). “Bacterial transport in NAPL-contaminated porous media.” *Journal of Environmental Engineering*, 126, 657–666.
- Saad, G. A. (2007). “Stochastic data assimilation with application to multi-phase flow and health monitoring problems.” Doctoral dissertation, University of Southern California, Los Angeles, CA.
- Saha, N., and Roy, D. (2009). “Extended kalman filters using explicit and derivative-free local linearizations.” *Applied Mathematical Modeling*, 33, 2545–2563.
- Salahshoor, K., Mosallaei, M., and Bayat, M. (2008). “Centralized and decentralized process and sensor fault monitoring using data fusion based on adaptive extended Kalman filter algorithm.” *Measurement Journal*, 41, 1059–1076.

- Samantaray, S. R., Dash, P. K., and Upadhyay, S. K. (2009). "Adaptive Kalman filter and neural network based high impedance fault detection in power distribution networks." *Electrical Power and Energy Systems*, 31, 167–172.
- Schwartz, F. W., and Zhang, H. (1994). *Fundamentals of groundwater*. John Wiley and Sons, Inc., New York.
- Spitz, K., and Moreno, J. (1996). *A practical guide to groundwater and solute transport Modeling*. John Wiley and Sons, Inc., New York.
- Tam, E. K. L., and Beyer, P. H. (2002). "Remediation of contaminated lands, a decision methodology for site owners." *Journal of Environmental Management*, 64, 387-400.
- Todd, A., Steve, B., Clint, D., Fredrik, S., Chong, W., and Mary, W. (1996) "Computational methods for multiphase flow and reactive transport problems arising in subsurface contaminant remediation." *Journal of Computational and Applied Mathematics*, 74, 19-32.
- Tompson, A. F. B., and Jackson, K. J. (1996). "Reactive transport in heterogeneous systems, an overview." *The Mineralogical Society of America*, 34, 269–310.
- U. S. Environmental Protection Agency (USEPA) (1985). "Protection of public water supplies from ground-water contamination." Center for Environmental Research Information, Cincinnati, OH.
- Walsh, M., Bryant, S., Schechter, R., and Lake, L. (1984). "Precipitation and dissolution of solids attending flow through porous media." *AIChE J.*, 30, 317-328.
- Warner, K. L. (2001). "Arsenic in glacial drift aquifers and the implication for drinking water, lower illinois river basin." *Ground Water*, 39(3), 433-442.

- Welch, A. H., Westjohn, D. B., Helsel, D.R., and Wanty, R. B. (2000). "Arsenic occurrence in ground water of the united states: occurrence and geochemistry." *Ground Water*, 38(4), 589-604.
- Welch, G., and Bishop, G. (2006). "An introduction to the kalman filter." *Tech. Rep. No.TR95-041*.University of North Carolina, Department of Computer Science,
http://www.cs.unc.edu/~welch/media/pdf/Kalman_intro.pdf. (assessed: July 20, 2012).
- Yu, Y. S., and Wenzhi, L. (1989). "Longitudinal dispersion in rivers: a dead zone model solution." *J. Am. Water Resour. Assoc.*, 25(2), 319–325.
- Zhang, H., and Zhao, Y. (2011) "The performance comparison and analysis of extended Kalman filters for GPS/DR navigation." *Optik*, 122, 777–781.
- Zheng, C., and Bennett, G. D. (1995). *Applied contaminant transport modeling, theory and practice*. Van Nostrand-Reinhold, New York, USA.
- Zou, S., and Parr, A. (1995). "Optimal estimation of two-dimensional contaminant transport." *Groundwater*, 33(2), 319–325.